Analysis of Polycyclic Aromatic Hydrocarbons in the Particulate Phase of Biomass Smoke by Mass Spectrometric Methods

by

Virginia L. Benefield

A Thesis Submitted in Partial Fulfillment of the Requirements for the Degree of Master of Science in Chemistry

Middle Tennessee State University

December 2021

Thesis Committee

Dr. Mengliang Zhang, Chair

Dr. Ngee Sing Chong

Dr. Chengshan Wang

Dedicated to the man who inspired me, encouraged me, and actually understood me. I Love you Pappy

ABSTRACT

Particulate matter (PM) from wildfire smoke is a great health concern for firefighters, who rarely wear full protective breathing equipment. Some of the most concerning particulate matter toxicants are polycyclic aromatic hydrocarbons and heavy metals. Polycyclic aromatic hydrocarbons (PAHs) are a class of compounds created by the incomplete combustion of organic materials. They are known as mutagens, carcinogens and have been known to cause heart disease. Traditionally gas chromatography-mass spectrometry (GC-MS) has been used to quantify the levels of PAHs, but this tends to be labor-intensive and time-consuming. This study describes a novel method for the PAH analysis by direct analysis in real-time-mass spectrometry (DART-MS). The proposed DART-MS method allows for the quantification of both polar and non-polar PAHs quickly with no labor-intensive extraction. DART-MS can potentially serve as an alternative method for the detection of PAHs in wildfire smoke, with higher throughput. The analysis of heavy metals in PM by inductively coupled plasma - optical emission spectrometry (ICP-OES) has also been implemented in this study.

TABLE OF CONTENTS

Page

Page

TABLE OF FIGURES

TABLE OF TABLES

Page

CHAPTER ONE: INTRODUCTION

1.1 Toxicants from Fire Smoke

In 2020 alone, over 10 million acres of land in the United States were burned in wildfire events, with California accounting for 38% of the total acres burned. In 2020, the total acres burned was well above the ten-year average[1], which corresponds to an upward trend in wildfire events. On average 27,000 Firefighters, each year are deployed to these fires[2]. These wildfire events pose serious health risks not only because of the inherent danger of the fire itself but also because of the toxicants from the smoke. These toxicants can include particulate matter released during the burning process. Particulate matter (PM) is considered the most prominent health hazard from wildfire smoke[3] consisting of gases, organic matter, metals, and dust or soil particles. Larger particles can irritate the nose, throat, and eyes; however, the most dangerous of these toxicants are particles smaller than 10 micrometers. This is because they can enter and irritate the lungs, but particles 2.5 micrometers or smaller, also typically referred to as $PM_{2.5}$, pose the greatest health threat[4]. $PM_{2.5}$ and smaller can pass past the terminal bronchioles into the alveolar region. $PM_{0.1}$ can pass through the alveolar surface, where they can be translocated to other organs[2]. Because of the ability of $PM_{2.5}$ and smaller to pass into the bloodstream, the health risk associated with these PMs is higher. These health risks include an acute decrease in lung function, cardiovascular disease, and pulmonary disease[5]. These toxicants have also been associated with carcinogenic effects[6]. This

translocation of PMs usually happens one to two days from exposure and depends on the dose of the PMs.[2]

During the Camp Fire in California, which burned for a total of 15 days in November of 2018 and burned more than 150,000 acres, the $PM_{2.5}$ levels were 100 times higher than the average at the most highly smoke polluted site, Chico, California[3]. There were also higher than normal levels of PMs in December and January that could be possibly attributed to this event. The worst of the effects of this fire only lasted for a day after the fire was extinguished, but during this time, the toxicant levels were comparable to China and India in their industrial centers. The level of PM seen at these industrial centers has been linked to high blood pressure, cancer, reproductive effects, and both learning deficiencies and behavioral changes in children. These countries have an increase in hospital visits due to respiratory and cardiac illnesses and infections. The U.S. Environmental Protection Agency (EPA) has estimated that between 1,500 and 2,500 deaths annually can be attributed to short-term exposure to $PM_{2.5}$ from wildfire smoke[3]. The long-term effects of being exposed to these toxicants year after year can include brain defects, including memory loss, depression, and learning disorders. They can also include the previously stated pulmonary diseases such as asthma and chronic obstructive pulmonary disease (COPD), as well as cardiac disease[3].

While the level of PM in wildfire smoke is of concern to civilians in the area of the active fire, the people most at risk of long-term health concerns are firefighters. This is due to the long hours fighting the blaze and the lack of protective respiratory equipment worn by the Firefighters. Previous studies have shown that Firefighters that regularly fight wildfires, such as those in California, are exposed to PM above

recommended yearly exposure limits[7]. This exposure is made more significant by the lack of formal regulations of respiratory personal protective equipment (PPE). Most PPE for woodland firefighters is to minimize heat stress injuries, and even these regulations were not formalized until 1977. Currently, there are no formal regulations on respiratory PPE for firefighters during a wildfire event[8]. When fighting a wildfire, Firefighters can be exposed to smoke and PM in several different ways including, when directly suppressing the fire, when constructing a fire line, when monitoring the fire line, and while patrolling the outskirts of the fire[2]. They can also be exposed during the cleanup of the fire, such as extinguishing smoldering material to avoid rekindling. The highest concentration exposure to PM is during the direct suppression stage[2]. The damage done by PM is made worse during this time due to the strenuous nature of direct suppression because nasal breathers will switch to oral-nasal breathing during hard labor. This causes less effective filtering of air and a higher deposit of toxicants in the distal airway[2]. During some wildfire events, respiratory protection may not be worn at all. This is particularly concerning to firefighters as even those fighting structural fires (wearing respiratory PPE) have twice the risk of malignant mesothelioma compared to the rest of the United States population[6].

Several studies have reported that the risk of upper respiratory infections increases with exposure to PM A study in China found that just short-term exposure to PM increased the hospitalizations for pneumonia[9]. Not only does the risk of contracting these infections increase but also the severity of the infection[2]. One study suggested that one of the causes of this increase of infection is the alteration of pulmonary macrophages when exposed to wood smoke[10]. This study showed that unlike a typical immune

response to other respiratory irritants such as cigarette smoke, exposure to wood smoke causes a depression of the microphage immune response[10]. Pulmonary macrophages are important in the adaptive and innate immune system when dealing with respiratory infections. Another possible reason for this increase in infection is thought to be caused by oxidative stress, which causes damage to the epithelial cells[2]. Exposure to PM is believed to have led to an increase in the rate of infection of SARS-CoV-2[2]. There are two hypotheses of why. The first is that the SARS-CoV-2 virus is absorbed into the PM, which promotes airborne transmission. This mode of transmission has been reported with other infections, including respiratory syncytial virus (RSV) and influenza A virus subtype (H5N1)[2]. The second hypothesis involves the change in gene expression of pulmonary cells when exposed to PM. When pulmonary epithelial cells are exposed to PM, they upregulate a protein receptor for the virus (angiotensin-converting enzyme II). Cigarette smokers have also been shown to have a similar upregulation. This could explain the higher rates of SARS-CoV-2 rates amongst smokers[2].

1.2 Polycyclic Aromatic Hydrocarbons

One particularly hazardous type of toxicant in PMs is polycyclic aromatic hydrocarbons (PAH). PAH is a class of compounds formed by two or more fused aromatic rings containing only carbon and hydrogen[11]. Some of the more dangerous PAHs are known carcinogens and mutagens. PAHs have also been used as dyes, medicines, plastics, pesticides[20]. Naphthalene is used as a dye, to make mothballs, explosives, lubricants, and plastics. Anthracene is used to make pesticides, wood preservatives, and dyes. These are both lower molecular weight PAHs.

The more dangerous PAHs have a high molecular weight. The smaller molecular weight PAHs are less hazardous by themselves but can react to nitrogen oxides and ozone to become highly toxic polar PAHs[12]. Typically, PAHs are solid, colorless crystals at room temperature and have decreasing volatility with increasing molecular weight[11]. They are also lipophilic with decreasing solubility in aqueous solutions with an increasing number of aromatic rings. Because of PAH's hydrophobicity, they can easily bind to air particulates and the soil, enabling them to persist in the environment.

PAHs are formed by the incomplete combustion of organic material and were one of the first pollutants found in the atmosphere to be carcinogenic[11]. PAHs are formed both by natural and anthropogenic causes. Natural causes include events such as volcanic activity and wildfires. Anthropogenic causes are created by humans, such as burning trash, fossil fuel, and tobacco[11]. The physical properties of PAHs make them mobile in the environment. They can use water, air, and soil to distribute themselves. Lighter-weight PAHs mainly exist in the gas phase in the atmosphere, while those with more than four aromatic rings mainly exist in the particulate phase[11]. Studies have also shown that there is a correlation between the amount of dust in the air and the amount of PAH in the particulate phase. More PAH exists in the gas phase in the summer, while in the winter, they exist more in the particulate phase[13]. The primary reason for PAH to be in the atmosphere is due to the burning of fossil fuels. The concentration of PAH from this source has been declining in most developed countries with the passage of clean air policies[11]. The concentration of PAH remains high in developing countries such as India due to air pollution from burning coal and other biomass. Humans who smoke and are occupationally exposed are mainly exposed to PAHs through polluted air being breathed

in. This contaminated air comes from cigarette smoke and work hazards, such as fuel combustion or open flames[11]. People who are non-smokers are mainly exposed to eating foods that have been smoked, grilled, or fried. These cooking processes can generate PAHs, particularly traditional smokers, where the smoke is not separated from the food. Food can also contain PAHs if it has been grown in contaminated soil[14]. Foods such as fish and other aquatic life readily absorb PAHs from contaminated water due to PAHs lipophilicity[15]. This lipophilicity also explains why the highest concentration of PAH in contaminated food is found in the fatty tissue of the organism[15]. Humans can also be exposed to PAHs if they come into contact with contaminated soil through dermal absorption[11].

The dangers of PAHs were first explored in the 1700s, but it wasn't until the mid-1900s that safety standards started to be implemented. The most comprehensive of these first safety standards were implemented by the Standard Oil Company in 1956. Some of these standards included restricting the number of employees exposed, supplying protective clothing, and removing the employee from exposure if a lesion appeared. While the safety standards of the 1950s did help protect workers, it wasn't until 1985 that the Occupational Safety and Health Administration (OSHA) set a maximum allowable amount of PAH exposure for an 8-hour workday ($0.2mg/m^3$)[16]. Several states have also established maximum allowable limits of the most dangerous PAHs in both groundwater and atmospheric for not only workers but for all citizens. The most commonly restricted PAH for each state is Benzo[a]pyrene, but Fluoranthene, Chrysene, and Benzo [a]anthracene are also included for some states[16]. In 1993, The EPA classified the following PAHs as possible human carcinogens: benzo[a]anthracene,

benzo[b]fluoranthene, benzo[j]fluoranthene, benzo[k]fluoranthene, benzo[a]pyrene, benzo[a,h]acridine, benzo[a,j]acridine, benzo[c,g]carbazole, dibenzo [a,e]pyrene, dibenzo [a,h]pyrene, and dibenzo[a,c]pyrene[16]. Most of these PAHs are included in this study, along with others. A full list can be found in table 1.

It has been a known fact that certain PAHs can cause cancer in animals for upwards of 200 years. In the 1970s, studies were done to understand the correlation between coke-oven emissions and workers getting lung cancer[16]. In 1981, a study connected benzo[a]pyrene with respiratory cancer in animals[17]. These cancers included tumors of the nasal passage, pharynx, trachea, larynx, and esophagus. The tumor types were squamous cell carcinoma, papillary polyps, and papillomas. Several other studies including mice and rats have shown clear links between exposure to PAHs and the morbidity rate of cancer. The location of the cancer is dependent on the type of exposure. Ingested PAH causes stomach cancer. Contaminated air causes lung cancer, and dermal exposure causes skin cancer.

PAHs are indirect-acting carcinogens. The most well-understood PAH is benzo[a]pyrene, and because of this, the metabolism of benzo[a]pyrene is a good model of how PAHs cause cancer in humans. Benzo[a]pyrene is metabolized to benzo[a]pyrene-7,8-dihydrodiol-9,10-epoxide (BPDE). BPDE is much more electrophilic than benzo[a]pyrene, and it can then covalently bind to the DNA. This forms a DNA adduct which disrupts the structure of DNA. If the repair enzymes cannot get rid of the adduct, it can lead to changes in the DNA. These changes can cause cancer, mutations, and tumors[18]. The adducts that BPDE usually form are deoxyadenosine or deoxyguanosine nucleotides. The mutations that are caused by this adduct typically involve the genes for

detection of DNA damage and repair. One of the proteins that are most dangerously affect is the P53 gene. This gene is a tumor-suppressing gene. The mutation of this gene has been seen in many forms of cancer but primarily in cancers of epithelial origin. There is a high correlation between the mutation of P53 and lung cancers. The concentration of these DNA adducts is highest one hour after exposure to benzo[a]pyrene. The repair mechanism does eliminate roughly half of these adducts, but after 24-48 hours, 40% of the adducts remained, according to one study[18].

Another way that PAHs cause damage is by introducing oxidative damage. CYP450 and other enzymes can transform PAHs into quinones that can bind to DNA and create more adducts or cause oxidative damage. These enzymes also cause PAHs to generate free radicals. This free radical damage causes tissue damage and can lead to heart disease. PAHs including benzo[a]pyrene have steroid-like structures and can act as endocrine disrupters. In this case, this causes low levels of androgen receptors which bind testosterone. Disruption of endocrine processes has also been linked with breast cancer.

Once exposure to PAHs occurs, they are quickly distributed through the body. They can be detected in tissues minutes to hours after exposure. Following the metabolism, PAHs are then excreted by the body. Acute effects of PAHs have not been observed in humans; however, in mice, acute exposure orally led to liver damage. Occupational exposure to PAHs has led to not just cancer but also lung damage, chest pain, cough, skin irritation, respiratory irritation, and a compromised immune system. There have also been reports studying the effect of benzo[a]pyrene on pregnant women. They concluded that benzo[a]pyrene can cross the placenta, and benzo[a]pyrene adducts have been found in fetal cord blood[19]. The presence of these adducts has also been

associated with lowered motor development in infants. In mice, exposure to benzo[a]pyrene has been correlated to lowered fertility and fetal death. Some studies suggest that benzo[a]pyrene could cause a neurotoxic effect on children and fetuses. The neurotoxic effects include impaired cognitive abilities, motor development, and attention deficits. There has also been a correlation between increased PAH exposure and anxiety and depression in adults[19].

The most at-risk populations are those that are being exposed to high levels of PAHs either by living near highly polluted areas or those exposed occupationally. A study that tracked children living near a coal power station showed that the children had twice the chance of having developmental delays by the age of two compared to other children[19]. In the United States due to the clean air act, the population greatest at risk are those who are exposed occupationally. This includes those who are exposed to soot, tar, or smoke dermally or through inhalation. The number of occupations included in the United States was once much higher than today, but because of OSHA, the rate of exposure has decreased in many of those occupations. Wildland firefighters remain at risk because as mentioned before, they are not required to wear protective respiratory gear while on duty.

All Firefighters have a higher exposure to PAHs than the typical occupation. This is due in part to dermal exposure. While Firefighters wear protective clothing during a fire, that protective clothing is removed without taking precautions to protect the skin from the soot and tar on them. There is also the problem that the equipment that Firefighters wear even in structural fires only has limited chemical resistance[21]. To make matters worse one study found that Firefighters more often than not were storing their

turnout gear in personal vehicles after a fire event[21]. This is directly against the National Fire Protection Association (NFPA) code 1851.9.1.6. which states, “contaminated gear must not be transported in the passenger compartment of a personal vehicle. If the gear is transported in the passenger compartment, the gear must be placed in a protective case or bag to prevent cross contamination”. The study determined this violation was particularly bad for volunteer Firefighters. The turnout gear that Firefighters wear now is much better than in the past, but it was still designed to protect them from fire and not airborne or dermal toxicants. These dangers exist for all firefighters but are exacerbated by the complete lack of, in most cases, breathing protection for wildland firefighters.

1.3 Heavy Metals

Another toxicant that is of concern after a wildfire event is heavy metals. Heavy metals are natural constituents of the soil and are needed for some plant life to survive[23]. These necessary for survival heavy metals include zinc, copper, iron, magnesium, and cobalt, to name a few[24]. Typically, in nature, these metals exist in small enough concentrations to be of no danger to human, animal, or plant life, and in fact, without these micronutrients animals and plants would die. Even though these elements are needed to sustain life, they can still be dangerous in high enough amounts. There are 23 heavy metals that are thought to be the most concerning. These include mercury, nickel, antimony, lead, arsenic, chromium, cadmium, and thallium, to name a few. Due to their human toxicity, the most often studied heavy metals are lead, mercury, cadmium, chromium, and arsenic. One of the most common ways these elements get into the

environment in rich enough amounts to be concerning is through pollution. Lead is often used in the production of batteries, ammunition, and fuel. Mercury and cadmium are often also used in batteries. Chromium and arsenic are used in the production of steel and metal alloys. The production of these items often leads to the leaching of these heavy metals into the environment. Pollution may be the leading cause of high concentrations of dangerous heavy metals in the soil and water, but it is not the only way for heavy metals to become dangerous. Besides pollution, heavy metals can enter the environment through erosion and natural weathering. While they are not introduced to the environment through wildfire events, they can be concentrated by a wildfire.

Heavy metals are always in the environment in low, non-dangerous concentrations, but after a wildfire event, they become concentrated in the ash[22]. Ash is mostly made up of hydroxides and oxides. The base cations of these are typically calcium, potassium, and magnesium but can include silica and phosphorus[22]. Ash can also contain heavy metals, depending on the biomass that is burned. This ash can then be deposited in water sources, in the soil, or onto humans nearby. Firefighters can be exposed to heavy metals in ash from wildfires by the ash being deposited onto their turnout gear and equipment. Other humans can be exposed to this contaminated ash during the cleanup processes. When the ash is deposited back into the soil or water sources, plants, animals, and people can be exposed, which can last generations. Plants absorb heavy metals through contaminated soil, air, and water. There are many routes for exposure to heavy metals, including contaminated air, ash, and water, but the most common way for the average person in the United States to be exposed to heavy metals is through eating vegetation with high concentrations of heavy metals[25].

The health effects of heavy metals are numerous. Many like arsenic are primary carcinogens[25]. Humans are typically exposed to arsenic through contaminated drinking water. Other heavy metals such as lead can damage plants by causing lipid membrane damage[25]. Lead in humans also causes oxidative stress, which can lead to cancer, neurogenerative disease, cardiovascular diseases, and asthma[25]. Many heavy metals such as lead can build up over time in humans and other organisms, causing chronic health problems. Mercury is another example of this. Mercury poisoning can also be acute, targeting the brain primarily, but any can be impaired[25]. Mercury is a neurotoxin and attacks the mitochondria, microtubules and causes lipid peroxidation[25]. Mercury poisoning remains an ongoing issue around the world. It is estimated that up to 10% of American women have mercury levels at a high enough to cause a neurological defect in any offspring they might have[26]. Cadmium also accumulates in the body throughout a person's lifetime. Cadmium is a by-product of zinc production, which is essential for growth in humans, animals, and plants. Any cadmium in the soil can remain there for decades. Plants absorb the cadmium and pass it along to animals that eat them. Cadmium poisoning can cause an iron deficiency by binding to certain ligands[25]. It can also cause nephrotoxicity, which damages the kidneys, and because zinc and cadmium have the same oxidative state, cadmium can replace zinc in the body.

Chromium is a heavy metal that is toxic to humans. It is not only released into the environment through pollution but also by sewage of animals. This heavy metal can also stay in soil deposits for generations. Trivalent chromium Cr(III) is naturally found in the environment at low levels and is relatively harmless. This is because of its weak membrane permeability. However, other forms of chromium such as hexavalent

chromium Cr(VI) can penetrate the cell membrane[25]. Hexavalent chromium is listed as a group one human carcinogen due to its mutagenic properties.

1.4 Analytical Methods for PAH and Heavy Metal Analysis

There are a few different methods for analyzing PAHs and heavy metals. The most common analytical methods include gas chromatography-mass spectrometry (GC-MS) and liquid chromatography-mass spectrometry (LC-MS) for the analysis of PAHs and for heavy metals atomic absorption spectroscopy (AAS) and inductively coupled plasma spectroscopy (ICP). The ICP can be coupled with a few different instruments one being mass spectrometry as with the LC and GC. It can also be coupled with optical emission spectroscopy (OES), which is the method used in this study. OES is used to determine the concentrations of trace amounts of 70 elements reliably.

Gas chromatography has traditionally been the most commonly used analytical technique to analyze PAHs, but liquid chromatography has also been utilized. GC-MS is often used because of the complexity of the PAH mixtures and the properties of the PAH themselves[27]. LC can be favored because of its superior separation efficiency and the fact that UV detectors can also be used to monitor PAHs. The type of sample also needs to be considered when determining the technique to use. If it is a water sample, then liquid chromatography would probably be the best course of action as there would be limited sample preparation. However, if the sample is on a filter, then the traditional GC method would be better.

1.4.1 EPA Methods

According to Environmental Protection Agency method 610: Polycyclic Aromatic Hydrocarbons, either high-performance liquid chromatography or gas chromatography can be used in the analysis of the following PAHs: acenaphthene, acenaphthylene, anthracene, benzo(a)anthracene, benzo(a)pyrene, benzo(b)fluoranthene, benzo(ghi)perylene, benzo(k)fluoranthene, chrysene, dibenzo(a,h)anthracene, fluoranthene, fluorene, indeno(1,2,3-cd)pyrene, naphthalene, phenanthrene, and pyrene[28]. This EPA method for GC does not adequately resolve all of the PAHs, but the LC method does resolve these all 16 PAHs. This method, however, is specific to water samples. EPA method TO-13A is for ambient air samples, which this study focuses on. This method is for gas chromatography-mass spectrometry only. For ambient air samples, the EPA suggests using GC-MS rather than LC-MS due to its selectivity, sensitivity, and its ability to separate PAHs in complex samples. The TO-13A method used XAD-2 sorbent tubes or PUF filters. The ambient air was drawn through the filter using an air sampler. The PAHs were extracted from the filter using Soxhlet extraction, which included the use of methylene chloride as the extraction solution, and the sample was concentrated using an evaporator. An internal standard mixture of D8-Naphthalene, D10-Acenaphthene, D10-Phenanthrene, D12-Chrysene, D12-Perylene was added. The sample is then cleaned using a silica gel, before GC-MS analysis. For the GC analysis, 2μL of the sample is injected into the instrument. The sample is injected at 250°C. The initial temperature was 70°C with a ramp rate of 10°C/min to 300°C. The interface temperature was 290°C. The total run time was approximately 50 minutes. Calibration curves were constructed using five-point calibrations.

1.4.2 Other methods

National Institute for Occupational Safety and Health (NIOSH) also has both GC-MS and LC-MS methods. The NIOSH GC-MS method is similar to the EPA method using a similar filter and sorbent tube. The sample collection included a 2 L/min flow rate for the pump being used to collect the ambient air. The injection temperature was 200°C with a temperature gradient of 30 to 290 °C at 4 °C/min. This method also suggested methylene chloride or acetonitrile as the extraction solvent. Both EPA and NIOSH recommend keeping the samples in a refrigerator as the more volatile PAH can be lost.

Other methods have followed similarly. One difference from a 2021 study used solid-phase microextraction[31]. The study developed a graphite-coated fiber that reduced the cleanup of the sample and preconcentrated the sample much better than the traditional commercially available poly(dimethyl siloxane) fiber. The reliability of this method had a relative standard deviation (RSD) of 4.2-9.5% and accuracy rates of between 80-110%[31]. This method may be a good alternative for trace PAH analysis.

1.5 Direct Analysis in Real Time-Mass Spectrometry

Direct analysis in real-time mass spectrometry (DART-MS) has become an important analytical technique for trace analysis since it came into use in the early 2000s. DART-MS has, until recently, been seen as a screening tool. However, advances in chemometrics and mass spectrometry have shown that this technique can be used for quantitative results. These advancements also include the use of solid-phase extraction (SPE) and thermal desorption. SPE allows the user to simplify complex mixtures, while the use of thermal desorption for the detection of less volatile components. The main

advantages to the DART-MS over more traditional methods such as GC-MS and LC-MS are the speed of analysis and the limited sample prep. DART-MS can analyze samples at ambient atmospheric conditions. Along with desorption electrospray ionization (DESI), which was introduced a few months after the DART, DART-MS was the first of the ambient atmospheric pressure ionization technique. Due to the sample being analyzed in the open atmosphere and being near ground potential, DESI, DART, and other related techniques are often referred to as ambient mass spectrometry[32]. The increase in popularity of the DART and DESI is in part due to the limited sample prep. In most cases, the sample has almost no pretreatment[32]. Because of this lack of pretreatment, the uses of DART are vast.

DART works by having an inert gas (usually helium or nitrogen) become metastable by flowing through a chamber where the gas encounters an electrical discharge. This creates electrons, ions, and excited state (metastable) atoms[33]. The majority of the charged molecules are removed by the grid. This leaves only the uncharged particles left, including the metastable atoms. The gas then passes through a second grid, which stops ion-ion recombination[33]. Next, the gas encounters the sample, where several ionization mechanisms can occur. The simplest is called Penning ionization[34]. This is where energy is transferred from the gas M^* to the sample molecule S, resulting in the ionization of the molecule (S^+). This also creates an electron (e-) and a neutral gas molecule (M)[34]. This is the dominant reaction when nitrogen is used as the inert gas.

$$M^* + S \longrightarrow S^+ + e^- + M$$

Helium is the most commonly used gas, and when helium is used the dominant reaction is involved in the ionization of water molecules (H_2O^+). Helium is the most commonly used inert gas due to other utilized gases not having enough energy to ionize the water molecules directly[35]. The mechanism also involves the transfer of a proton along with the ionization of water[35].

1. $He^* + H_2O \longrightarrow He + H_2O^+ + e^-$
2. $H_2O^+ + H_2O + e^- \longrightarrow H_3O^+ + OH^-$
3. $H_3O^+ + nH_2O \longrightarrow [(H_2O)_{n+1} + H]^+$
4. $S + [(H_2O)_{n+1} + H]^+ \longrightarrow [S+H]^+ + (H_2O)_{n+1}$

DART-MS has been used extensively in forensic science research, especially in drug analysis[35]. It has also been used in toxicology research and to identify explosives, gunpowder residue, fire debris, ignitable liquids, inks, and paints[35]. DART-MS has also been demonstrated to be of use in other applications such as the identification and classification of plant, insect, animal fragments, and environmental and food samples[36]. The major advantage of DART-MS for these samples is the ability to directly analyze these samples with little to no sample prep. Drugs can be analyzed both in pill form and in powder and laid directly onto a heating stage, as can other samples.

In this study, GC-MS, ICP-OES, and DART-MS are utilized to analyze both PAHs and heavy metals found in the particulate phase of wildfire smoke. GC-MS as the traditional method for analyzing PAH was used to quantify and identify 18 non-polar PAHs and 7 polar PAHs. The DART-MS, as a novel method was used to

quantify and identify those same PAHs. The results of the GC-MS and the DART-MS were compared. The ICP-OES was used to identify and quantify the heavy metal concentration in wildfire smoke.

CHAPTER TWO METHODS AND MATERIALS

2.1. Materials and Reagents

2.1.1. PAH Related

To prepare standard samples and to optimize the GC-MS and DART-MS methods, AccuStandard's Expanded PAH mix (2.0mg/mL in dichloromethane: benzene) was used for the non-polar PAHs. For the polar PAHs, 1mg of the solid of the polar PAH was dissolved in methylene chloride (D37-4 Fisher Chemical). The polar PAHs are 2-naphthol (Sigma-Aldrich 185507-5G), 1-naphthol (Sigma-Aldrich N1000-10G), 1-nitronaphthalene (TCI N02120, 9-fluorenone (Sigma-Aldrich F1506-5G-A), 1-nitropyrene (ChemCruz sc-251528), 2-nitrofluorene (Santa Cruz Biotechnology sc-230598), 1-hydroxypyrene (TCI H1435), and 1,2-Benzanthraquinone (TCI B0018). As an internal standard for the GC-MS, a PAH surrogate cocktail (200 μg/mL in CD2CL2/CH3OD 50:250, ES2044) from Cambridge Isotope Laboratories was used. For the DART-MS as an internal standard, 9-bromophenathrene (Alfa Aesar L09033) solid dissolved in methylene chloride to 1mg/mL was used. For the non-polar dust samples, A certified reference material (ERM-CZ100), and for polar dust samples, the dissolved polar compounds were spiked at the needed concentrations onto 8632 ultra-fine test dust from NIST.

2.1.2. Heavy Metal Related

A certified reference sample (ERM-CZ120) from ERM was used for the heavy metal analysis.

2.1.3. Filter Related

Two different filters were tested to determine which had better efficiency for extraction and they are the Omega PTFE filter and PALLFLEX quartz filter from SKC. The SKC quartz filter was selected, and two sizes of this quartz filter were used for analysis. The two sizes were a 37-mm $PM_{2.5}$ filter and a 25-mm $PM_{<10}$ filter. All of the filters were weighed on a Mettler Toledo microbalance (XPR6UD5).

2.2 Instruments and Parameters

2.2.1. GC-MS

To characterize non-polar PAHs found in the particulate phase of wildfire smoke, gas chromatography (GC-2010 Shimadzu) was used in tandem with mass spectrometry (GCMS-QP2010S). The injection temperature was 270 °C. The start temperature was 100 °C, which was held for 2 minutes. The temperature was then raised by 8 °C/min to 210 °C and then 2 °C/min to 280 °C. Finally, the temperature was raised by 17 °C/min to 340 °C and held at 340 °C for 6 minutes. The total run time for this method was 60.28 minutes.

The original method was run using a full scan mode; however, this method was not sensitive enough, so the final method used selected ion monitoring (SIM) mode. SIM was used to monitor 11 ions for the non-polar PAHs and 12 ions for the polar PAHs. The ions for the non-polar PAH were *m/z* 121, 142, 152, 153, 165, 178, 202, 228, 252, 276, and 278. While the ions for the polar PAH were *m/z* 115, 144, 127, 173, 180, 165, 208, 152, 202, 258, 230, and 201. The ions 136, 160, 188, 212, 264, and 288 were also added to this method to monitor the internal standards. A total of 18 non-polar compounds and 7 polar compounds were detected using this method.

2.2.2. DART-MS

To analyze polar and non-polar PAHs using DART-MS, the other half of the filter was used. A 5mm hole was punched out of the filter and then analyzed by DART-MS directly. Five μL of an internal standard (8-Bromophenatrene) with a concentration of 500 ng/mL was spiked onto the filter and let dry for 5 minutes. The filter was then placed onto a copper pot, which was on a thermal desorption device. The following temperature gradient was used. The start temperature was 30 °C, which was held for 12 seconds. The temperature was then raised by 100 °C/min until 600 °C. This was then held for 30 seconds. The desorbed chemicals were then detected by the DART-MS.

Because the distribution of PAH on the filter was unknown and only a small amount of the filter was being analyzed, the PAH distribution on the filter was studied. This was done by creating a small backyard fire and collecting the smoke with two pumps. This was repeated for a total of four samples. The larger filter had three 5mm holes punched out: one was in the middle, one was on the edge, and the last was directed between the two other holes. The smaller filter had four holes punched out: one was directly over the concentrated dark spot of smoke debris, one was in the center of the filter, one was on the outer edge, and the final hole was directly between two of the four dark spots.

2.2.3. ICP-OES

The following heavy metals were analyzed on the Agilent 5800 ICP-OES: Al, As, Be, Cd, Co, Cr, Cu, Fe, Hg, Mn, Ni, Pb, Se, V, Zn. An Agilent SPS 4 Autosampler was also employed.

2.3 Sample Preparations

2.3.1. Preparation of Different Samples for GC-MS

Before the extraction, the filters were cut in half. Half of the filter was stored while the other half was used in the extraction. Fifty μL of the internal standard was added and allowed to dry on the bench for ten minutes. The filter half was placed in 10 mL of an extraction solution (methanol and methylene chloride 1:2, *v/v*). The solution was then vortexed for 20 seconds and then sonicated for 20 minutes. It was then vortexed again, and the filter was removed. The solution was then dried using nitrogen evaporation. It was then reconstituted using 2 mL of the extraction solution, and vortexed again for 20 seconds. The solution was filtered using a syringe filter (Celltreat: nylon 0.22 μm 13 mm diameter), and 200 μL of the filtered solution was removed for the analysis of both polar and non-polar PAHs using GC-MS.

2.3.2. Preparation of Different Samples for ICP-OES

Two extraction methods were compared for the heavy metal analysis using the ICP-OES. The first method was a hot plate method. For this method, ¼ of the filter was placed in 3 mL of concentrated HCl for 5 minutes. Then, 2 mL of concentrated nitric acid (BDH3044-500MLPC from VWR Chemicals) was added. This was left for one hour. The mixture with the filter was then placed onto a hot plate set at 140°C covered by a watch glass for 10 minutes. The watch glass was removed, and the solution was left on the hot plate until about 1 mL of solution was left. The solution was removed from the heat and allowed to cool to room temperature. After it had cool, 5 mL of concentrated HCL (ACS grade BDH3026-500MLP from VWR Chemicals) were added, and the sides of the beaker were rinsed with a 1:9 HNO_3: water solution. The solution was then heated to near

boiling and allowed to cool for 30 minutes. The solution was quantitatively transferred to a 10 mL volumetric flask and QS with a 1:9 HCl solution.

The second method of preparation was microwave extraction. For this method, ¼ of a filter was placed in the microwave extraction container. Then, 5 mL of concentrated nitric acid were added. The container was then placed in the Anton Paar MW5000 microwave digestion system. The temperature was set to 180 ℃ and was held for 15 minutes. The container was then removed, and 5 mL of hydrochloric acid was added. The container was then placed back into the microwave and the same procedure was followed. The container was then removed from the microwave and quantitatively transferred into a 50 mL volumetric flask and Q.S. with a 1:9 solution of nitric acid solution.

2.4 Method Validation for GC-MS and DART-MS

2.4.1. Calibration

For the GC-MS, a six-point calibration curve was created. The concentrations used to create this curve were 0.02 μg/mL, 0.05 μg/mL, 0.1 μg/mL, 0.2 μg/mL, 0.5 μg/mL, and 1 μg/mL. For the DART-MS, a five-point calibration curve was created using the concentrations of 0.05 μg/mL, 0.1 μg/mL, 0.2 μg/mL, 0.5 μg/mL, and 1 μg/mL. For the ICP-OES a six-point calibration curve was created using the concentrations of 0.2 ppm, 0.5 ppm, 1 ppm, 5 ppm, 10 ppm, and 20 ppm. All calibration samples were analyzed in triplicate.

2.4.2. Accuracy and Precision

Accuracy and precision were evaluated for both the GC-MS and the DART-MS methods. To analyze the accuracy and precision, three concentrations were selected. A known amount of both the polar and non-polar PAHs was spiked onto a filter. The PAHs were then extracted using the above method. The samples were then analyzed using both DART-MS and GC-MS. These concentrations were 0.05 μg/mL, 0.2 μg/mL, and 0.5 μg/mL for both GC-MS and DART-MS and were run in triplicate.

2.4.3. Recovery

The recovery was performed similarly using the same parameters as accuracy and precision. The known concentrations of analytes on the filters were compared against the samples without filters. The analysis was also performed in triplicate.

2.4.4. Validation

Certified dust samples were analyzed to certify the methods. About 0.005 g of certified dust was weighed out onto a filter. The filter was cut in half and half the sample was used for GC-MS analysis and the other half for DART-MS analysis. The sample was then extracted and analyzed using the GC-MS method. The other half was analyzed using the DART-MS method. The results from both analyses were compared to the known concentrations and to each other.

2.5 Sample Collection

Samples were collected from both prescribed fires and real wildfire events. The prescribed fires were fires that were intentionally set for collecting of PM. The wildfire events were created either naturally or by other sources and not for the purpose of this project.

2.5.1. Sampling device and parameters

The SKC AirCheck XR5000 sample pump with a personal modular impactor (SKC PM coarse) was used in all collections. The airflow was set a 3 L/min. The collection time varied between sample collections. The pumps were either set up on tripods or hung from a Firefighters' belt.

2.5.2. Field Sample Collection

The field samples were collected in California. These samples were collected from live wildfire events, using the sampling devices and parameters listed in section 2.5.1. The first set of samples were collected during the fall of 2020. The samples were collected during two wildfire events, the Silverado fire, which burned from October 26, 2020, till November 7, 2020, and the Bond fire, which burned from December 2, 2020, till December 10, 2020. Three sampling sites were used all of which had varying distances from the fires. The first site was 4.0 miles from the fires. The second site was 8.0 miles from the fires, and the third site was 26.5 miles from the fires. All three sampling sites from the fall of 2020 were collected in the same way, on tripods for 12 hours.

The second set of field samples were collected during the fall of 2021. This set of data was collected on August 10, 2021, and September 13, 2021, at the site of the fire. The samples from September 13 were collected during the staging of the equipment, and the samples from August 10 were collected during the fighting of the fire. The filters from both sample sets were put into filter holders and shipped to Tennessee for analysis.

2.5.3. Live Fire Sample Collection

The live-fire samples were collected in Tennessee. These samples were collected with the help of both the Mount Pleasant Fire Department and the Murfreesboro Fire and Rescue Department. Both sets of data were collected during the summer of 2021. The first set of data was collected in Murfreesboro, TN. This burn was a prescribed burn that was set using wooden boards placed inside an enclosed fire training building. Two PM sampling pumps were set up on tripods, while the other two pumps were worn by the Firefighters controlling the burn. The sampling lasted about 10 minutes which including activities of firing, staging, and attacking.

The second prescribed fire took place in Mount Pleasant, TN. This fire took place outdoors. The burning material consisted of biomass common to Middle Tennessee, including branches, leaves, and grass. One pump was placed onto a tripod about 10 feet away from the fire, while two pumps were worn by Firefighters controlling the fire. The three pumps collected samples for one hour. No accelerant was used to start either fire.

2.5.4. Small Scale Fire Sample Collection

Small scale fires were set to further develop the methods for the GC-MS and the DART-MS. These fires were set in small aluminum cans. Holes were placed in the bottoms of these cans for better airflow. Biomass common to Middle Tennessee, such as pine needles, leaves, and dried grasses, was placed in the can and lit using a lighter with no accelerant. The samples were collected using three pumps placed in a triangle formation on tripods around the can. The pumps were placed about 2 feet above the fire. The samples were collected over one hour.

CHAPTER FOUR RESULTS AND DISCUSSION

3.1 Method Development

3.1.1. Evaluation of Filters

In order to optimize the extraction of PAH, two types of filters were tested, an Omega PTFE filter and a PALLFLEX quartz filter. These filters were tested using the selected GC-MS method and non-polar PAH. The PALLFLEX quartz filter was able to extract all 18 non-polar compounds (table 1), but it was less efficient at extraction for more volatile compounds than the PTFE filter (table 2). The Omega PTFE filter however was unable to extract three of the 18 non-polar compounds. The Omega PTFE filter overall was less efficient for the extraction of PAHs using the selected extraction method. Because of this, the PALLFLEX quartz filter was selected as the filter for this project.

Table 1. Percent of non-polar PAH extracted from PALLFLEX quartz filter

Quartz Filter Recovery	
Compound name	% Extracted
Naphthalene	36.2
2-Methynaphthalene	43.1
1-Methynaphthalene	41.8
Acenaphthylene	64.2
Acenaphthene	71.9
Fluorene	74.2
Phenanthrene	94.6
Anthracene	98.6
Fluoranthene	98
Pyrene	92.7
Benzo (a) anthracene	99.6
Chrysene	100.8
Benzo (b) fluoranthene	43.9
Benzo (k)fluoranthene	77.1
Benzo (a) pyrene	78.6
Indeno (1,2,3-cd) pyrene	89
Dibenzo (a,h) anthracene	94.9
Benzo (g,h,i) perylene	89.3

Table 2. Percent of non-polar PAH extracted from PTFE filter

Omega PTFE Filter Recovery	
Compound name	% Extracted
Naphthalene	53.4
2-Methynaphthalene	below calibration
1-Methynaphthalene	below calibration
Acenaphthylene	below calibration
Acenaphthene	58.3
Fluorene	63.1
Phenanthrene	76.4
Anthracene	92.1
Fluoranthene	79.9
Pyrene	75.2
Benzo (a) anthracene	73.9
Chrysene	101.7
Benzo (b) fluoranthene	81.3
Benzo (k)fluoranthene	82.1
Benzo (a) pyrene	80.4
Indeno (1,2,3-cd) pyrene	71.6
Dibenzo (a,h) anthracene	65.2
Benzo (g,h,i) perylene	71.7

3.1.2. Optimization of the GC-MS method

The GC-MS method was optimized to lower the limit of detection and to enhance separation. The first method tried was a 20-minute method, which had poor separation of the larger molecular weight compounds. This method had a start temperature of 80°C, held for 2 minutes, and raised to 280 °C by a rate of 17 °C/min. The second method was a 53-minute method, which had better separation. It had a start temperature of 100 °C, which was held for 2 minutes and then raised to 210 °C by a rate of 8 °C/min. Finally, the temperature was raised to 280 °C by a rate of 2 °C/min. While this method had better separation than the first method, both of these methods only eluted 15 of the 18 non-polar PAH. The three PAH that were not eluted were indeno(1,2,3-cd) pyrene, dibenzo(a,h)anthracene, benzo(g,h,i)perylene. These three PAHs have a higher molecular weight and are less volatile. Because of this, a final method was developed based on the 53-minute method. After the temperature of 280 °C was achieved, the temperature was raised again to 340 °C by a rate of 17°C/min and held for 6 minutes. This eluted the last three compounds. The final hurdle was that the detection limit using this method was not low enough. The full scan mode was changed to selective ion monitoring mode (SIM) to overcome this issue. SIM was used to monitor 11 ions for the non-polar PAH and 12 ions for the polar PAH. The ions for the non-polar PAH were *m/z* 121, 142, 152, 153, 165, 178, 202, 228, 252, 276, and 278. While the ions for the polar PAH were *m/z* 115, 144, 127, 173, 180, 165, 208, 152, 202, 258, 230, and 201. The internal standards were added

to correct for variability due to sample treatment and instrument variation. The ions 136, 160, 188, 212, 264, and 288 were used to monitor the internal standards. A total of 18 non-polar compounds and 7 polar compounds were detected using this method. Table 1 list the non-polar PAHs with their selected ions and retention times, and Table 2 lists the polar PAHs with their selected ions and retention times. Figure 1 lists the non-polar and polar compounds along with their retention times. It also lists whether the EPA classifies it as a priority pollutant.

Table 3. The table below lists the non-polar PAHs with their selected ions for monitoring and retention times.

Non-polar PAHs' Selected Ions with Retention Times		
Compound name	*m/z*	Retention time Range
Naphthalene	128	6.7-6.85
2-Methynaphthalene	142	8.5-8.7
1-Methynaphthalene	142	8.9-9.1
Acenaphthylene	152	11.6-11.8
Acenaphthene	153	12.0-12.2
Fluorene	165	13.6-13.8
Phenanthrene	178	17.0-17.2
Anthracene	178	17.2-17.4
Fluoranthene	202	23.0-23.2
Pyrene	202	24.7-25.0
Benzo (a) anthracene	228	35.2-35.5
Chrysene	228	35.7-36.0
Benzo (b) fluoranthene	252	46.1-46.4
Benzo (k)fluoranthene	252	46.4-46.7
Benzo (a) pyrene	252	49.7-50.0
Indeno (1,2,3-cd) pyrene	276	55.1-55.2
Dibenzo (a,h) anthracene	278	55.2-55.4
Benzo (g,h,i) perylene	276	56.0-56.2

Table 4. The table below lists the polar PAHs, their selected ions, and retention times.

Polar PAHs' Selected Ions with Retention Times		
Compound name	*m/z*	Retention time
2-Naphthol	144	12.4-12.9
1-Naphthol	144	12.9-13.5
Nitronaphthalene	173	14.1-14.4
9-Fluorenone	180	16.1-16.5
1,2-Benzanthraquinone	258	40.0-40.5
1-Hydroxpyene	189	33.5-33.8
2-Nitrofluorene	165	13.2-13.5

Polar and Non-polar PAHs Chromatograph

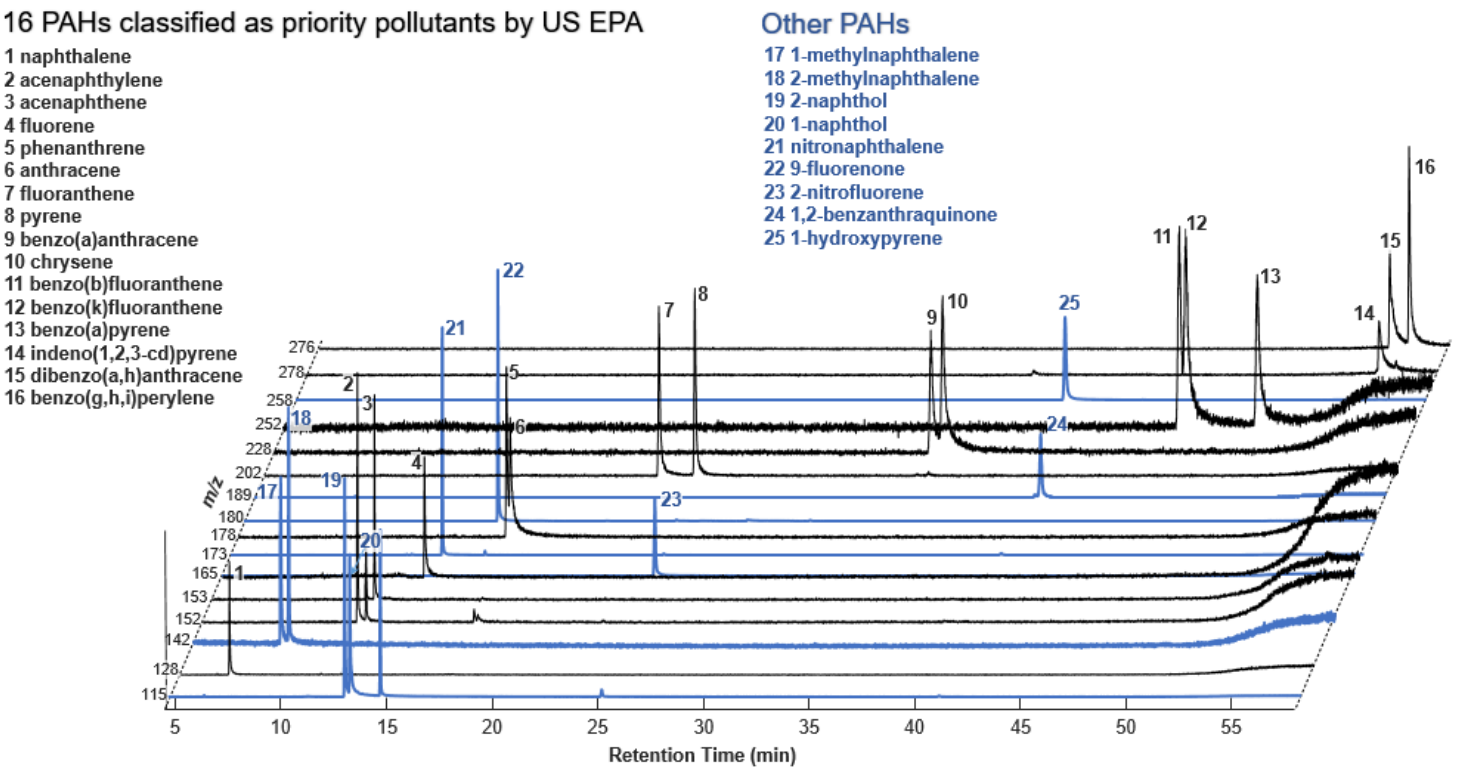

Figure 1. The figure above shows the 25 non-polar and polar PAHs that were analyzed with this method along with their retention times. 1-18 are the non-polar compounds and 19-25 are the polar compounds.

3.1.3. DART-MS method

The DART-MS method was also optimized. Both positive and negative modes were tested. The negative mode did not work well for the polar PAH. Mild separation was achieved for both polar and non-polar compounds using a temperature gradient, but coelution of similar analytes such as naphthene, 1-methylnaphthalene, and 2-methylnaphthalene is inevitable. Selected ions were used to monitor the PAHs. Tables 5 and 6 lists the polar and non-polar PAHs, their retention times, and their selected ions, respectively. Figure 2 shows the retention times and the selected ions for non-polar and polar PAH using the positive mode with the thermal desorption DART-MS method.

Table 5. The table below lists the polar PAHs, their selected ion, and Desorption Time for DART-MS analysis.

Polar PAHs' DART-MS Selected Ions and Desorption Times		
Compound name	*m/z*	Desorption time
2-Naphthol 1-Naphthol	145	0.72
9-Fluorenone	181	0.83
9,10-Phenatrequione	209	1.43
2-Nitrofluorene	212	1.19
1-Nitropyrene	248	1.54
1,2-Benzanthraquinone	259	1.53

Table 6. List the non-polar PAHs, their selected ion, and Desorption time for DART-MS analysis.

Non-polar PAHs' DART-MS Selected Ions and Desorption Times		
Compound name	*m/z*	Desorption time
Phenanthrene Anthracene	179	1.23
Fluoranthene Pyrene	203	1.4
Benzo(a)anthracene Chrysene	229	1.72
Benzo(b)Fluoranthene Benzo(k)Fluoranthene Benzo(a)pyrene	253	1.96
Indeno (1,2,3-cd) pyrene Benzo (g,h,i) perylene	277	2.16
Dibenzo(a,h)anthracene	279	2.21

Polar and Non-polar PAHs Desorption Times for DART-MS

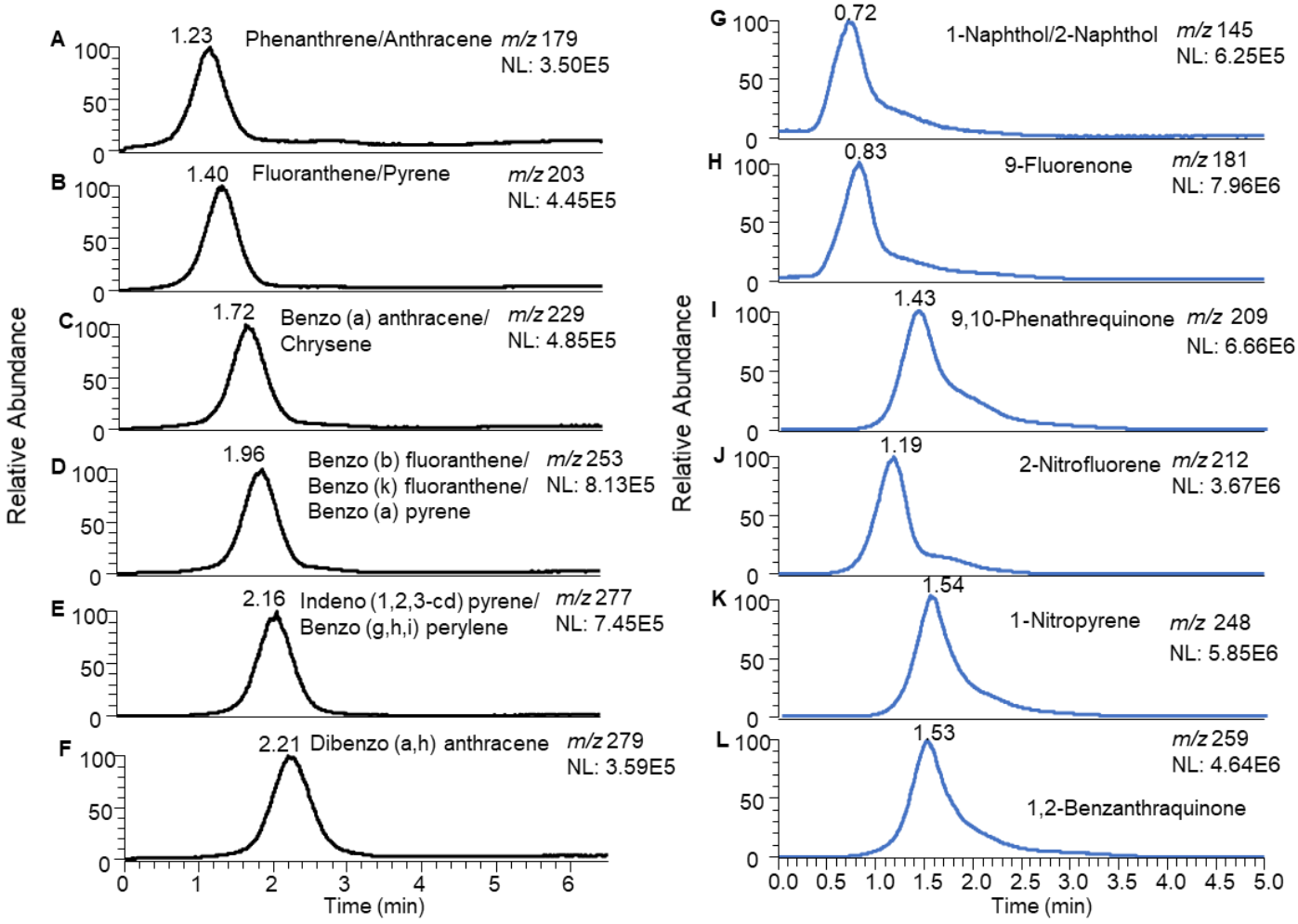

Figure 2. The desorption times and selected ions for the non-polar PAHs (left) and polar PAHs (right) for the DART-MS method.

3.2 PAH GC-MS Method Validation

3.2.1 Calibration

Calibration curves were constructed for all 18 non-polar PAH and all 7 of the polar PAH. These were constructed by using a ratio of the peak area of PAHs and its internal standard. Table 7 lists the non-polar PAH, their regression equation, and their R^2 value.

Table 8 list the polar PAH, their linear formula, and their R^2 value. Figures 3 and 4 show the examples of the calibration curves for naphthalene (a non-polar PAH) and 2-naphthol (a polar PAH).

Table 7. The table below lists the non-polar PAHs, their dynamic ranges, regression equations, and R^2 values.

Non-polar PAHs' Calibration			
Analyte	Dynamic Range (µg/mL)	Regression Equation	R^2
Naphthalene	0.05-1	y = 2.2555x+0.0577	0.9989
2-methynaphthalene	0.05-1	y = 0.9449x-0.0185	0.9982
1-Methynaphthalene	0.05-1	y = 1.5478x+0.0294	0.9984
Acenaphthylene	0.05-1	y = 3.3006x+0.0491	0.9989
Acenaphthylene	0.05-1	y = 1.5001x+0.0425	0.9988
Fluorene	0.05-1	y = 0.7918x-0.0209	0.998
Phenanthrene	0.05-1	y = 2.0825x-0.0512	0.9969
Anthracene	0.05-1	y= 1.9829x+0.2509	0.9804
Fluoranthene	0.05-1	y= 2.0056x+0.035	0.9987
Pyrene	0.05-1	y= 2.2866x+0.0306	0.999
Benzo (a) anthracene	0.05-1	y= 0.2416x-0.0113	0.9829
Chrysene	0.05-1	y= 1.6331x+0.0798	0.9975
Benzo (b) Fluoranthene	0.05-1	y= 1.1668x+0.7848	0.996
Benzo (k) fluoranthene	0.05-1	y= 1.4937x+1.041	0.9948
Benzo (a) pyrene	0.05-1	y= 0.7759x+1.0483	0.997
Indeno (1,2,3-cd) Pyrene	0.05-1	y= 1.8979x-0.0879	0.9921
Dibenzo (a,h) anthracene	0.05-1	y= 1.9965x+0.9429	0.9937
Benzo (g,h,i) perylene	0.05-1	y= 3.4831x+0.6133	0.9923

Table 8. The table below lists the polar PAH, the dynamic range, the regression equation, and the R^2 value for each PAH.

Polar PAHs' Calibration			
Analyte	Dynamic Range (µg/mL)	Regression equation	R^2
2-naphthol	0.02-1	y = 0.412x-0.0002	0.9964
1-naphthol	0.02-1	y=1.2855x-0.0633	0.9951
nitronaphthalene	0.02-1	y=0.92x-0.0066	0.993
9-Fluorenone	0.02-1	y=3.5505x-0.279	0.9936
2-Nitrofluorene	0.02-1	y=0.9083x-0.0106	0.9897
1-Hydroxpyrene	0.02-1	y=0.1841x+0.1785	0.9948
1,2-Benzanthraquinone	0.02-1	y=0.9525x-0.0439	0.9862

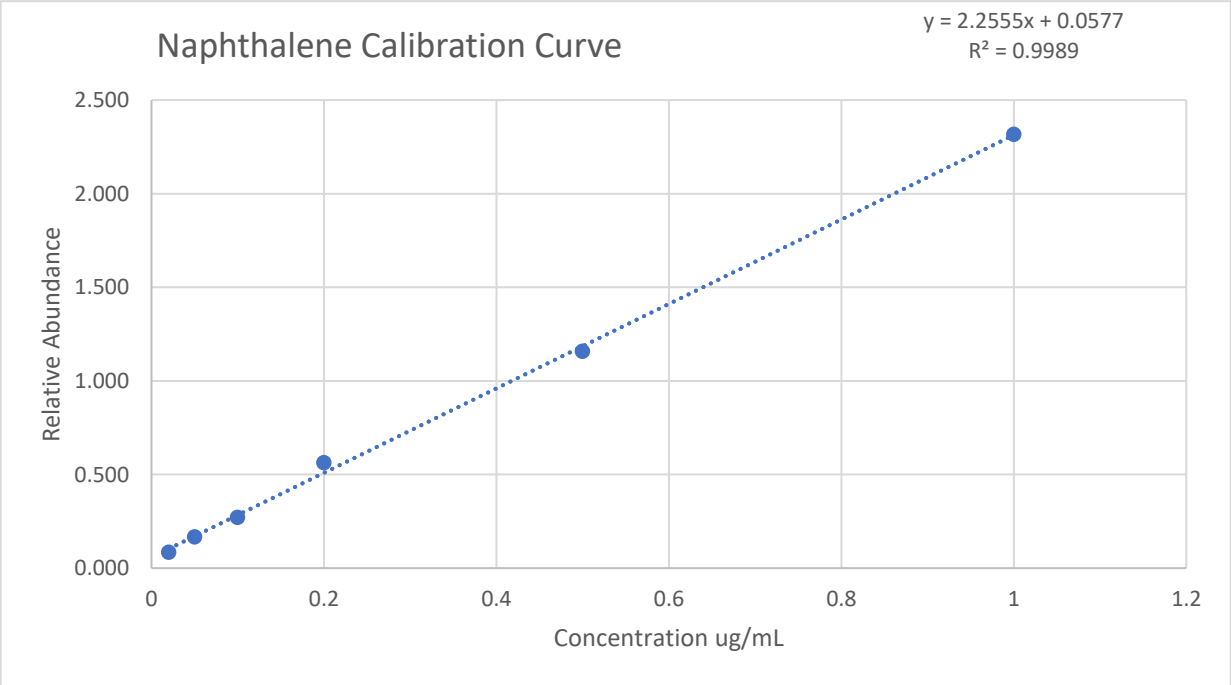

Figure 3. The calibration curve for Naphthalene, a non-polar PAH. It also shows the R^2 value and linear formula.

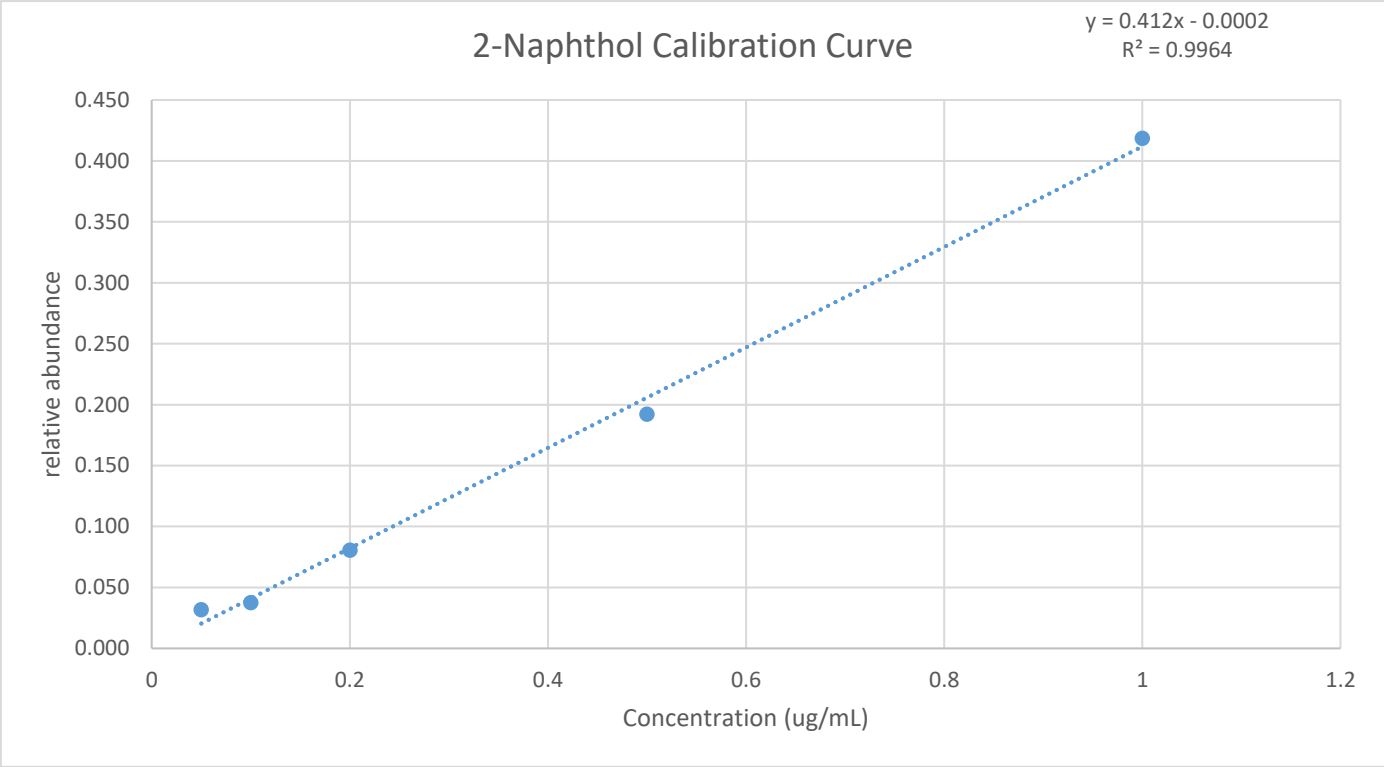

Figure 4. The calibration curve for 2-Naphthol, a polar PAH. It also shows the R^2 value and linear formula.

3.2.2 Accuracy and Precision

To test the accuracy and precision of this method, the concentrations of 0.1 µg/mL, 0.5 µg/mL, and 1 µg/mL PAH standard solutions were spiked onto half a filter in triplicate, and the previous extraction method was used to extract the PAHs. The optimized GC-MS method was then used to analyze the sample. Table 9 lists the non-polar PAHs' accuracy in percent relative error (RE) and precision in percent relative standard deviation (RSD). Table 10 lists the polar PAHs' accuracy in percent relative error and precision in percent relative standard deviation. Except for a few outliers, the polar and non-polar PAHs'

accuracies and precisions all fall less than 15%. This shows that the reproducibility of this method is good.

Table 9. The table below lists the non-polar PAH, the percent relative error for the accuracy, and the percent relative standard deviation for the precision.

Non-polar PAH Accuracy and Precision for GC-MS				
Analyte	Spiked Conc. (µg/mL)	Mean Calculated	Accuracy (RE %)	Precision (RSD %)
Naphthalene	0.1	0.1	11.2	11.8
	0.5	0.5	-6.1	1.5
	1	0.9	-7.0	9.7
2-Methynaphthalene	0.1	0.1	49.4	9.4
	0.5	0.5	9.7	7.3
	1	1.2	16.9	10.7
1-Methynaphthalene	0.1	0.1	48.8	10.4
	0.5	0.6	11.4	1.7
	1	1.1	12.6	12.5
Acenaphthylene	0.1	0.1	11.9	13.5
	0.5	0.5	-2.5	13.1
	1	1.0	-1.0	9.8
Acenaphthene	0.1	0.1	19.0	9.8
	0.5	0.4	-14.5	5.0
	1	0.9	-8.2	13.3

Table 9. Cont. The table below lists the non-polar PAH, the percent relative error for the accuracy, and the percent relative standard deviation for the precision.

Non-polar PAH Accuracy and Precision for GC-MS (Continued)				
Analyte	Spiked Conc. (µg/mL)	Mean Calculated	Accuracy (RE %)	Precision (RSD %)
Fluorene	0.1	0.1	36.6	3.0
	0.5	0.5	-0.5	10.8
	1	1.1	6.6	12.1
Phenanthrene	0.1	0.1	37.4	7.4
	0.5	0.6	17.0	0.8
	1	1.1	6.1	11.8
Anthracene	0.1	0.1	11.1	18.5
	0.5	0.5	-2.9	1.4
	1	1.1	11.1	9.7
Fluoranthene	0.1	0.1	18.0	14.2
	0.5	0.5	5.3	2.1
	1	1.1	8.6	8.1
Pyrene	0.1	0.1	45.9	5.8
	0.5	0.6	14.5	1.0
	1	1.1	13.0	7.4

Table 9. Cont. The table below lists the non-polar PAH, the percent relative error for the accuracy, and the percent relative standard deviation for the precision.

Non-polar PAH Accuracy and Precision for GC-MS (Continued)				
Analyte	Spiked Conc. (µg/mL)	Mean Calculated	Accuracy (RE %)	Precision (RSD %)
Benzo (a) anthracene	0.1	0.2	65.9	15.3
	0.5	0.7	30.5	1.3
	1	1.1	11.4	4.1
Chrysene	0.1	0.1	21.0	2.5
	0.5	0.5	4.0	7.7
	1.0	0.9	-6.9	8.2
Benzo (b) Fluoranthene	0.1	0.1	13.2	17.6
	0.5	0.5	-6.8	9.4
	1.0	1.1	6.4	12.8
Benzo (k) fluoranthene	0.1	0.1	5.2	10.5
	0.5	0.5	0.4	14.0
	1.0	1.0	-4.4	6.5
Benzo (a) pyrene	0.1	0.1	13.0	33.2
	0.5	0.5	2.6	16.5
	1.0	1.2	24.7	9.9

Table 9. Cont. The table below lists the non-polar PAH, the percent relative error for the accuracy, and the percent relative standard deviation for the precision.

Non-polar PAH Accuracy and Precision for GC-MS (Continued)				
Analyte	Spiked Conc. (µg/mL)	Mean Calculated	Accuracy (RE %)	Precision (RSD %)
Indeno (1,2,3-cd) Pyrene	0.1	0.2	51.4	7.3
	0.5	0.5	7.3	11.1
	1.0	1.0	3.8	17.5
Dibenzo (a,h) anthracene	0.1	0.1	3.5	10.4
	0.5	0.5	-1.5	16.2
	1.0	1.1	5.9	19.9
Benzo (g,h,i) perylene	0.1	0.1	10.3	20.0
	0.5	0.5	-0.6	7.4
	1.0	1.0	-1.4	15.3

Table 10. The table below lists the polar PAH, the percent relative error for the accuracy, and the percent relative standard deviation for the precision. These are averages of the three concentrations in triplicate.

Polar PAHs' Accuracy and Precision for GC-MS				
Analyte	Spiked Conc. (µg/mL)	Mean Calculated	Accuracy (RE %)	Precision (RSD %)
2-Naphthol	0.1	0.1	-35.2	9.8
	0.5	0.6	15.1	6.3
	1.0	1.1	11.9	6.6
1-Napthol	0.1	0.1	2.1	2.9
	0.5	0.5	3.2	1.2
	1.0	1.1	9.1	12.6
Nitronaphthalene	0.1	0.1	2.2	33.0
	0.5	0.5	3.6	9.1
	1.0	1.1	8.6	5.6
9-Fluorenone	0.1	0.1	-10.1	5.4
	0.5	0.5	-2.4	8.8
	1.0	1.1	8.0	8.9
2-Nitrofluorene	0.1	0.1	-9.7	17.1
	0.5	0.5	1.9	6.4
	1.0	1.1	10.8	20.7

Table 10. Continued The table below lists the polar PAH, the percent relative error for the accuracy, and the percent relative standard deviation for the precision. These are averages of the three concentrations in triplicate.

Polar PAHs' Accuracy and Precision for GC-MS Continued				
Analyte	Spiked Conc. (µg/mL)	Mean Calculated	Accuracy (RE %)	Precision (RSD %)
8-Bromophenatrene	0.1	0.1	9.5	8.8
	0.5	0.5	-7.2	11.7
	1.0	1.0	3.0	9.1
Benanthraquinone	0.1	0.1	10.7	14.9
	0.5	0.5	-0.6	1.2
	1.0	1.1	6.1	11.4
1-Hydroxpyrene	0.1	0.1	20.0	13.0
	0.5	0.5	1.7	4.3
	1.0	1.0	1.5	9.8

3.2.3. Recovery

The recovery for the polar and non-polar PAH was evaluated similarly to as it was done for accuracy and precision. The known concentrations of analytes on the filters were compared against the samples without filters. Table 11 list the average recoveries for non-polar PAHs, Table 12 list the average recoveries for polar PAHs. The average percent recovery for the non-polar PAHs was 111.8% with a standard deviation of 11.3.

The average percent recovery of the polar PAHs was 104.3 % with a standard deviation of 9.6. Except for a few outliers, the recovery percent is within 10% of 100% and has a standard deviation of less than 15%.

Table 11. The table below lists the average recovery percent and the average standard deviation (STDEV) of non-polar PAHs for the three spiked concentrations.

Non-polar PAHs' Recovery for GC-MS			
Analyte	Spiked Conc. (µg/mL)	Recovery %	STDEV %
Naphthalene	0.1	111.2	13.1
	0.5	93.9	1.4
	1.0	93.0	9.0
2-methylnaphthalene	0.1	149.4	14.0
	0.5	109.7	8.0
	1.0	116.9	12.5
1-Methylnaphthalene	0.1	148.8	15.4
	0.5	111.4	1.9
	1.0	112.6	14.1
Acenaphthylene	0.1	111.9	15.2
	0.5	97.5	12.8
	1.0	99.0	9.7
Phenanthrene	0.1	119.0	11.6
	0.5	85.5	4.3
	1.0	91.8	12.2

Table 11. Continued The table below lists the non-polar PAH, their average recovery percent for the three concentrations, and average standard deviation for the three concentrations in triplicate.

Non-polar PAHs' Recovery for GC-MS Continued			
Analyte	Spiked Conc. (µg/mL)	Recovery %	STDEV %
Fluorene	0.1	136.6	4.1
	0.5	99.5	10.8
	1.0	106.6	12.9
Phenanthrene	0.1	137.4	10.2
	0.5	117.0	1.0
	1.0	106.1	12.5
Anthracene	0.1	111.1	20.6
	0.5	97.1	1.4
	1.0	111.1	10.8
Fluoranthene	0.1	118.0	16.7
	0.5	105.3	2.2
	1.0	108.6	8.8
Pyrene	0.1	145.9	8.5
	0.5	114.5	1.1
	1.0	113.0	8.4

Table 11. Continued The table below lists the non-polar PAH, their average recovery percent for the three concentrations, and average standard deviation for the three concentrations in triplicate.

Non-polar PAHs' Recovery for GC-MS Continued			
Analyte	Spiked Conc. (µg/mL)	Recovery %	STDEV %
Benzo (a) anthracene	0.1	165.9	25.4
	0.5	130.5	1.6
	1.0	111.4	4.6
Chrysene	0.1	121.0	3.1
	0.5	104.0	8.0
	1.0	93.1	7.7
Benzo (b) Fluoranthene	0.1	113.2	19.9
	0.5	93.2	8.7
	1.0	106.4	13.6
Benzo (k) fluoranthene	0.1	105.2	11.0
	0.5	100.4	14.1
	1.0	95.6	6.2
Benzo (a) pyrene	0.1	113.0	37.5
	0.5	102.6	16.9
	1.0	124.7	12.3

Table 11. Continued The table below lists the non-polar PAH, their average recovery percent for the three concentrations, and average standard deviation for the three concentrations in triplicate.

Non-polar PAHs' Recovery for GC-MS Continued			
Analyte	Spiked Conc. (µg/mL)	Recovery %	STDEV %
Indeno (1,2,3-cd) Pyrene	0.1	151.4	11.0
	0.5	107.3	11.9
	1.0	103.8	18.2
Dibenzo (a,h) anthracene	0.1	103.5	10.7
	0.5	98.5	15.9
	1.0	105.9	21.1
Benzo (g,h,i) perylene	0.1	110.3	22.1
	0.5	99.4	7.3
	1.0	98.6	15.1

Table 12. The polar PAH, their average recovery for the three concentrations, and the average standard deviation for the three concentrations in triplicate.

Polar PAHs' Recovery for GC-MS			
Analyte	Spiked Conc. (μg/mL)	Recovery %	STDEV %
2-Naphthol	0.1	64.8	6.4
	0.5	115.1	7.3
	1.0	111.9	7.3
1-Napthol	0.1	102.1	2.9
	0.5	103.2	1.2
	1.0	109.1	13.8
Nitronaphthalene	0.1	102.2	33.7
	0.5	103.6	9.5
	1.0	108.6	6.1
9-Fluorenone	0.1	89.9	4.9
	0.5	97.6	8.6
	1.0	108.0	9.6
2-Nitrofluorene	0.1	90.3	15.4
	0.5	101.9	6.5
	1.0	110.8	22.9

Table 12. Continued The polar PAH, their average recovery for the three concentrations, and the average standard deviation for the three concentrations in triplicate.

Polar PAHs' Recovery for GC-MS Continued			
Analyte	Spiked Conc. (µg/mL)	Recovery %	STDEV %
8-Bromophenatrene	0.1	109.5	9.6
	0.5	92.8	10.9
	1.0	103.0	9.4
Benanthraquinone	0.1	110.7	16.5
	0.5	99.4	1.2
	1.0	106.1	12.1
1-Hydroxpyrene	0.1	120.0	15.6
	0.5	101.7	4.4
	1.0	101.5	10.0

3.2.4. Validation

Certified dust with three concentrations in triplicate of non-polar PAHs was analyzed. Table 13 lists the non-polar PAHs, their percent recovery, and the standard deviation. The average percent recovery for the certified dust sample of non-polar PAH was 104.8 with a standard deviation of 7.5. Overall, the results indicate that no substances significantly influence the recovery of the PAHs on the filters and in the dust samples.

Table 13. The table below lists the percent recovery for non-polar PAHs along with the standard deviation for the three concentrations in triplicate.

Non-polar PAH Dust Validation for GC-MS			
Analyte	Spiked Conc. (µg/mL)	Recovery %	STDEV %
Naphthalene	0.5	99.8	6.8
	0.2	113.7	4.2
	0.1	101.6	8.4
2-methylnaphthalene	0.5	99.7	10.3
	0.2	97.6	2.2
	0.1	96.8	7.2
1-Methylnaphthalene	0.5	103.9	5.2
	0.2	92.8	2.5
	0.1	103.5	14.4
Acenaphthylene	0.5	97.5	9.0
	0.2	96.4	3.3
	0.1	83.1	6.6
Acenaphthene	0.5	101.5	4.1
	0.2	111.5	10.2
	0.1	113.8	9.4

Table 13. Continued The table below lists the percent recovery for non-polar PAHs along with the standard deviation for the three concentrations in triplicate.

Non-polar PAH Dust Validation for GC-MS Continued			
Analyte	Spiked Conc. (µg/mL)	Recovery %	STDEV %
Phenanthrene	0.5	105.7	6.6
	0.2	105.1	8.7
	0.1	116.2	16.1
Fluorene	0.5	98.2	6.0
	0.2	102.3	2.1
	0.1	133.4	9.1
Anthracene	0.5	97.9	10.1
	0.2	108.7	7.5
	0.1	124.5	7.4
Fluoranthene	0.5	96.2	12.0
	0.2	100.3	9.4
	0.1	106.7	17.5
Pyrene	0.5	103.6	4.9
	0.2	106.0	6.1
	0.1	113.2	16.8

Table 13. Continued The table below lists the percent recovery for non-polar PAHs along with the standard deviation for the three concentrations in triplicate.

Non-polar PAH Dust Validation for GC-MS Continued			
Analyte	Spiked Conc. (µg/mL)	Recovery %	STDEV %
Benzo (a) anthracene	0.5	103.6	1.7
	0.2	103.2	3.3
	0.1	110.1	5.0
Chrysene	0.5	102.6	3.7
	0.2	105.4	4.7
	0.1	108.4	15.6
Benzo (b) Fluoranthene	0.5	100.6	6.1
	0.2	98.9	9.5
	0.1	110.6	8.6
Benzo (k) fluoranthene	0.5	98.8	1.6
	0.2	99.1	3.9
	0.1	115.1	1.7
Benzo (a) pyrene	0.5	100.5	8.6
	0.2	102.3	4.8
	0.1	106.3	13.8

Table 13. Continued The table below lists the percent recovery for non-polar PAHs along with the standard deviation for the three concentrations in triplicate.

Non-polar PAH Dust Validation for GC-MS Continued			
Analyte	Spiked Conc. (µg/mL)	Recovery %	STDEV %
Indeno (1,2,3-cd) Pyrene	0.5	103.4	2.5
	0.2	103.9	6.7
	0.1	118.6	10.3
Dibenzo (a,h) anthracene	0.5	98.9	11.2
	0.2	109.7	13.3
	0.1	103.7	5.5
Benzo (g,h,i) perylene	0.5	105.2	4.3
	0.2	100.2	8.4
	0.1	118.3	4.6

3.3 PAH DART-MS Method Development and Validation

3.3.1. Calibration

Calibration curves were created for each of the isomers for all the non-polar and polar PAHs. These were constructed using the peak areas of the extracted ion for the PAHs and the extracted ion of the internal standard used (8-Bromophenatrene). Tables 14 and 15 lists the non-polar and polar PAHs with their linear dynamic range, R^2 value, and linear

equation. Figure 5 shows the calibration curve for phenanthrene and anthracene, with a molecule weight of 178. Figure 6 shows the calibration curve for 1-nitropyrene.

Table 14. The table below lists the non-polar PAH analyzed with DART-MS, their linear range, regression equation, and R^2 value.

Non-polar PAHs' Calibration for DART-MS			
Analyte	Dynamic Range µg/mL	Regression equation	R^2
Acenaphthylene, Acenaphthene	0.05-1	y = 0.5075x+0.0289	0.9872
Fluorene	0.05-1	y=0.2037x+0.1769	0.9894
Phenanthrene, Anthracene	0.05-1	y=2.5794x+0.7882	0.9911
Fluoranthene, Pyrene	0.05-1	y=6.007x+1.6656	0.986
Benzo(a) anthracene, Chrysene	0.05-1	y=7.021x+1.3967	0.9947
Benzo(b) fluoranthene, Benzo(k) fluoranthene, Benzo (a)pyrene	0.05-1	y=12.573x+2.6386	0.9933
Indeno(1,2,3-cd) pyrene, Benzo(g,h,i) perylene	0.05-1	y=9.9246x+1.7352	0.995
Dibenzo (a,h) anthracene	0.05-1	y=5.1677x+1.3961	0.9944

Table 15. The table below lists the polar PAH analyzed with DART-MS, their linear range, regression equation, and R^2 value.

Polar PAH Calibration for DART-MS			
Analyte	Linear Dynamic Range (µg/mL)	Regression equation	R^2
2-naphthol,1-naphthol	0.05-1	y = 1.5154x+0.0904	0.9829
1-nitropyrene	0.05-1	y=21.413x-0.2596	0.9995
9-Fluorenone	0.05-1	y=9.0943x-0.2644	0.996
1,2-Benzoanthraquinone	0.05-1	y=15.764x+0.1701	0.9944
2-nitrofluorene	0.05-1	y=9.3353x-0.3213	0.9974
9,10-phenanthrenequinone	0.05-1	y=1.9215x+0.5496	0.9881

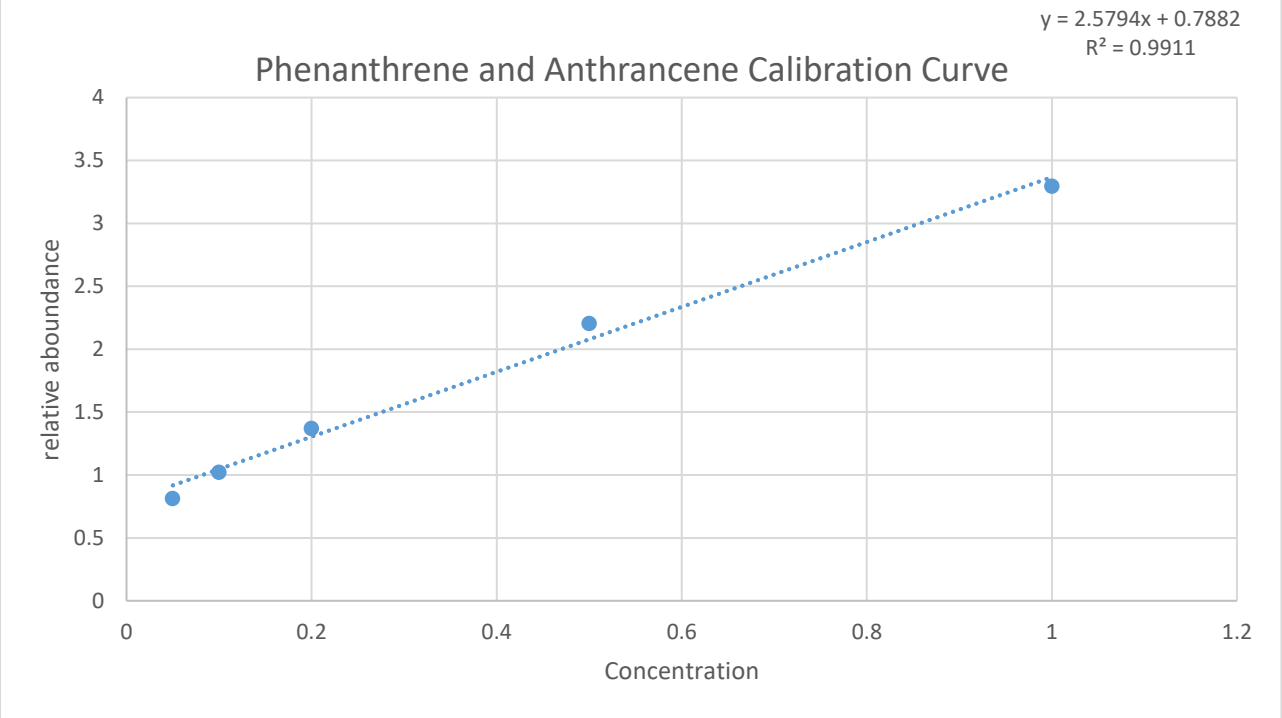

Figure 5. The figure above shows the calibration curve for both Phenanthrene and anthracene along with the regression equation and R^2 value.

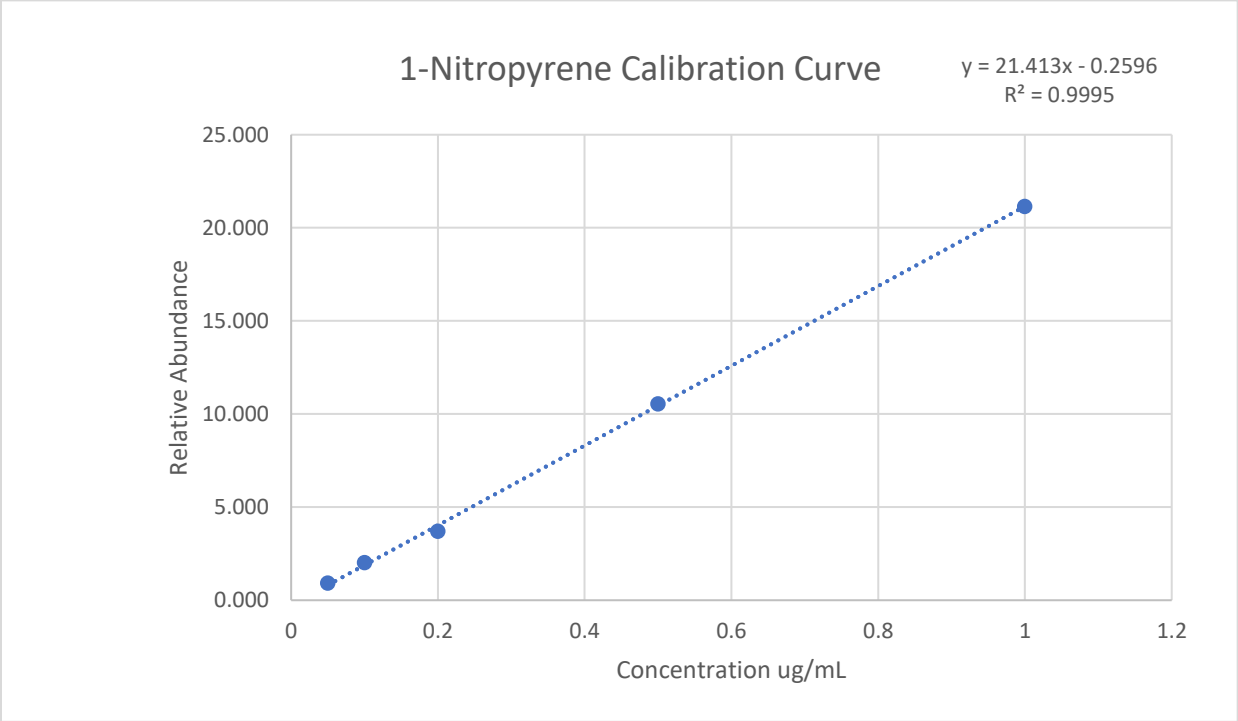

Figure 6. The figure above is the calibration curve for 1-nitropyrene. It also shows the regression equation and the R^2 value.

3.3.2. Accuracy and Precision

Three concentrations of PAHs were chosen at 0.5 µg/mL, 0.2 µg/mL, and 0.1 µg/mL for the evaluation of accuracy and precision. These concentrations were analyzed in triplicate using the DART-MS method. A 5mm hole was punched out of a quartz filter, placed onto a copper pot, 5 µL of the PAH standard solution was spiked onto the filter, and it was allowed to dry for 5 minutes. The filter was then analyzed using the DART-

MS method. Table 16 lists the average accuracy in percent relative error and the precision in percent relative standard deviation for the non-polar PAHs. Table 17 lists the average accuracy in percent relative error and the precision in percent relative standard deviation for the polar PAHs. Except for a few, the polar and non-polar PAHs have accuracies and precisions below 20%, with several having accuracies and precisions below 15%, showing good accuracy and precision.

Table 16. The table below lists the non-polar PAH, their average recovery percent for the three concentrations, and average standard deviation for the three concentrations in triplicate for the DART-MS method.

Non-polar PAH Accuracy and Precision for DART-MS				
Analyte	Spiked Conc. (µg/mL)	Mean Calculated	Accuracy (RE %)	Precision (RSD %)
Acenaphthylene, Acenaphthene	0.5	0.6	18.0	8.6
	0.2	0.3	73.3	10.5
	0.1	0.1	7.9	6.9
Fluorene	0.5	0.5	1.6	7.2
	0.2	0.2	9.3	13.9
	0.1	0.1	31.1	8.1
Phenanthrene Anthracene	0.5	0.5	6.8	3.0
	0.2	0.2	18.8	5.4
	0.1	0.1	22.0	31.5
Fluoranthene Pyrene	0.5	0.5	4.0	9.0
	0.2	0.2	20.9	4.8
	0.1	0.1	11.2	11.6

Table 16. Continued The table below lists the non-polar PAH, their average recovery percent for the three concentrations, and average standard deviation for the three concentrations in triplicate for the DART-MS method.

Non-polar PAH Accuracy and Precision for DART-MS Continued				
Analyte	Spiked Conc. (µg/mL)	Mean Calculated	Accuracy (RE %)	Precision (RSD %)
Benzo(a) anthracene Chrysene	0.5	0.5	-1.9	11.3
	0.2	0.3	28.4	10.1
	0.1	0.1	-2.1	17.5
Benzo(b) fluoranthene Benzo(k) fluoranthene Benzo (a)pyrene	0.5	0.5	6.7	5.2
	0.2	0.2	11.0	9.3
	0.1	0.1	-5.7	9.2
Indeno(1,2,3-cd) pyrene, Benzo(g,h,i) perylene	0.5	0.6	14.7	2.1
	0.2	0.2	23.5	10.7
	0.1	0.1	16.2	20.3
Dibenzo (a,h) anthracene	0.5	0.5	3.9	18.6
	0.2	0.3	26.6	18.5
	0.1	0.1	-2.1	24.6

Table 17. The table below lists the polar PAH, their recovery percent, and standard deviation for the three concentrations in triplicate for the DART-MS method.

Polar PAH Accuracy and Precision for DART-MS				
Analyte	Spiked Conc. (µg/mL)	Mean Calculated	Accuracy (RE %)	Precision (RSD %)
2-naphthol 1-naphthol	0.5	0.4	-15.7	12.0
	0.2	0.2	12.2	36.3
	0.1	0.1	-10.1	34.2
nitropyrene	0.5	0.5	-5.5	16.7
	0.2	0.2	-10.4	5.1
	0.1	0.1	-1.7	5.6
9-fluorenone	0.5	0.4	-15.5	7.7
	0.2	0.2	-14.1	11.7
	0.1	0.1	11.7	21.5
1,2- Benzanthraquinone	0.5	0.5	6.7	6.3
	0.2	0.2	-23.0	11.3
	0.1	0.1	-1.5	12.7

Table 17. Continued The table below lists the polar PAH, their recovery percent, and standard deviation for the three concentrations in triplicate for the DART-MS method.

Polar PAH Accuracy and Precision for DART-MS Continued				
Analyte	Spiked Conc. (µg/mL)	Mean Calculated	Accuracy (RE %)	Precision (RSD %)
1-nitrofluorene	0.5	0.5	-9.8	5.8
	0.2	0.2	-3.9	15.6
	0.1	0.1	0.7	5.1
9,10-phenanthrenequinone	0.5	0.6	10.2	7.8
	0.2	0.3	53.3	16.3
	0.1	0.1	7.2	15.8

3.3.3. Recovery

Table 18 lists the average recoveries for non-polar PAHs, and Table 19 lists the average recoveries for polar PAHs. Most of the polar and non-polar PAHs have recoveries within 20% of 100% and have standard deviations below 20%, showing good recovery rates for this method considering the lack of sample preparation.

Table 18. The table below lists the percent recovery for non-polar PAHs along with the standard deviation for the three concentrations in triplicate.

Non-polar PAH Recovery for DART-MS			
Analyte	Spiked Conc. (μg/mL)	Recovery %	STDEV %
Acenaphthylene, Acenaphthene	0.5	118.0	10.1
	0.2	173.3	18.2
	0.1	107.9	7.4
Fluorene	0.5	101.6	7.3
	0.2	109.3	15.2
	0.1	131.1	10.6
Phenanthrene Anthracene	0.5	106.8	3.2
	0.2	118.8	6.4
	0.1	122.0	38.4
Fluoranthene Pyrene	0.5	104.0	9.4
	0.2	120.9	5.8
	0.1	111.2	12.9

Table 18. Continued The table below lists the percent recovery for non-polar PAHs along with the standard deviation for the three concentrations in triplicate.

Non-polar PAH Recovery for DART-MS Continued			
Analyte	Spiked Conc. (µg/mL)	Recovery %	STDEV %
Benzo(a) anthracene Chrysene	0.5	98.1	11.1
	0.2	128.4	13.0
	0.1	97.9	17.1
Benzo(b) fluoranthene Benzo(k) fluoranthene Benzo (a)pyrene	0.5	106.7	5.5
	0.2	111.0	10.3
	0.1	94.3	8.6
Indeno(1,2,3-cd) pyrene, Benzo(g,h,i) perylene	0.5	114.7	2.5
	0.2	123.5	13.2
	0.1	116.2	23.5
Dibenzo (a,h) anthracene	0.5	103.9	19.3
	0.2	126.6	23.5
	0.1	97.9	24.1

Table 19. The table below lists the average percent recovery for polar PAHs along with the standard deviation for the three concentrations in triplicate.

Polar PAH Recovery for DART-MS			
Analyte	Spiked Conc. (µg/mL)	Recovery %	STDEV %
2-naphthol 1-naphthol	0.5	84.3	10.1
	0.2	112.2	40.7
	0.1	89.9	30.8
nitropyrene	0.5	94.5	15.8
	0.2	89.6	4.6
	0.1	98.3	5.5
9-fluorenone	0.5	84.5	6.5
	0.2	85.9	10.1
	0.1	111.7	24.0
1,2-Benzanthraquinone	0.5	106.7	6.7
	0.2	77.0	8.7
	0.1	98.5	12.5

Table 19. Continued The table below lists the average percent recovery for polar PAHs along with the standard deviation for the three concentrations in triplicate.

Polar PAH Recovery for DART-MS Continued			
Analyte	Spiked Conc. (µg/mL)	Recovery %	STDEV %
1-nitrofluorene	0.5	90.2	5.2
	0.2	96.1	15.0
	0.1	100.7	5.1
9,10- phenanthrenequinone	0.5	110.2	8.6
	0.2	153.3	25.0
	0.1	107.2	17.0

3.3.4. Validation

To Validate this DART-MS method, certified dust with three concentrations in triplicate of non-polar PAH were analyzed. Table 20 lists the non-polar PAHs, their percent recovery, and the standard deviation. The average percent recovery for the certified dust sample of non-polar PAH was 103.0% with a standard deviation of 13.4%. Overall, the results indicate that no substances significantly influence the recovery of the PAHs on the filters and in the dust samples.

Table 20. The table below lists the percent recovery for non-polar PAHs along with the standard deviation for the three concentrations in triplicate for the DART-MS method.

Non-polar PAH Dust Validation for DART-MS			
Analyte	Spiked Conc. (μg/mL)	Recovery %	STDEV %
Acenaphthylene, Acenaphthene	0.5	90.8	1.9
	0.2	114.9	8.3
	0.1	112.8	16.9
Fluorene	0.5	104.5	6.0
	0.2	107.5	8.7
	0.1	95.5	9.0
Phenanthrene Anthracene	0.5	109.6	6.5
	0.2	101.8	17.8
	0.1	104.7	24.8
Fluoranthene Pyrene	0.5	106.7	4.0
	0.2	115.1	17.2
	0.1	84.8	14.2

Table 20. Continued The table below lists the percent recovery for non-polar PAHs along with the standard deviation for the three concentrations in triplicate for the DART-MS method.

Non-polar PAH Dust Validation for DART-MS Continued			
Analyte	**Spiked Conc. (µg/mL)**	**Recovery %**	**STDEV %**
Benzo(a) anthracene Chrysene	0.5	97.9	9.2
	0.2	111.5	25.6
	0.1	105.3	27.4
Benzo(b) fluoranthene Benzo(k) fluoranthene Benzo (a)pyrene	0.5	98.2	13.9
	0.2	103.2	15.4
	0.1	94.6	16.9
Indeno(1,2,3-cd) pyrene, Benzo(g,h,i) perylene	0.5	108.8	9.2
	0.2	101.5	13.9
	0.1	107.1	9.4
Dibenzo (a,h) anthracene	0.5	101.6	4.8
	0.2	98.3	13.5
	0.1	96.5	26.8

3.4 Results of Filter Sample Analysis

3.4.1. PAH filter distribution

When removing the filters from the filter holders, it was noticed on the 25mm filter that the PM was not evenly distributed throughout the filter. There were four darker circles of PM concentrated on the filters due to the way that the impactor was designed. When analyzing the sample by the GC-MS, this uneven concentration was not a problem as the concentration was symmetrical and the entire half filter was used for the extraction; however, when analyzing the sample by the DART-MS, where only a 5mm hole was punched out, it was important to determine the percent of PAH on the filter in various places. Two small-scale fire experiments were performed. Two sampling devices were used to collect samples from a small-scale fire on August 6, 2021; two different devices were used on August 7, 2021. This gave a total of four samples for the 25mm filters and four samples for the 37 mm filters. After the samples were collected, four 5 mm holes were punched out of the 25 mm sample, and three holes were punched out of the 37 mm sample. Figure 7 shows the placement of these holes for the 25 mm filter, and figure 8 shows the placement of the 37 mm holes. Figure 9 shows the percent of non-polar PAH on the 25 mm filter. Figure 10 shows the percent of non-polar PAH on the 37 mm filter. As can be seen in Figure 9 spot D, which was the darkest portion of the filter had 35% of the total PAH on the filter, while spot B had 30%. The darkest spot had the most PAH as expected, but spot B also had a high percentage due to its placement close to two of the dark spots. Spots O and M both had less than 20% because they were further away from

the dark spots. Figure 10 shows that the 37 mm filter had the highest concentration at the center of the filter and as the edges were approached the concentration lessened slightly.

Placement of hole on 25mm filter

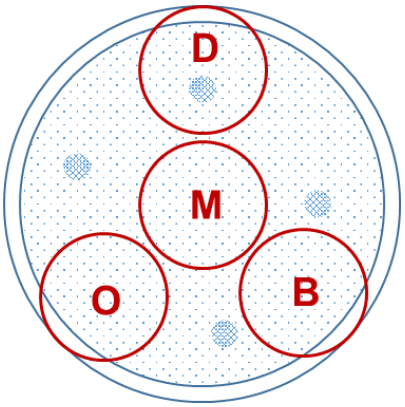

Figure 7. The figure above shows the placement of the holes that were punched out for analysis on the 25mm filter.

Placement of hole on 37mm filter

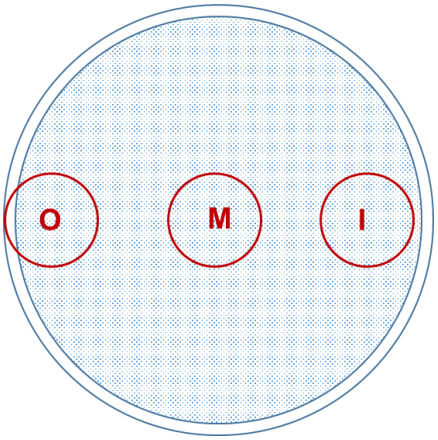

Figure 8. The figure above shows the placement of the holes that were punched out for analysis on the 37mm filter.

25mm Filter Distribution

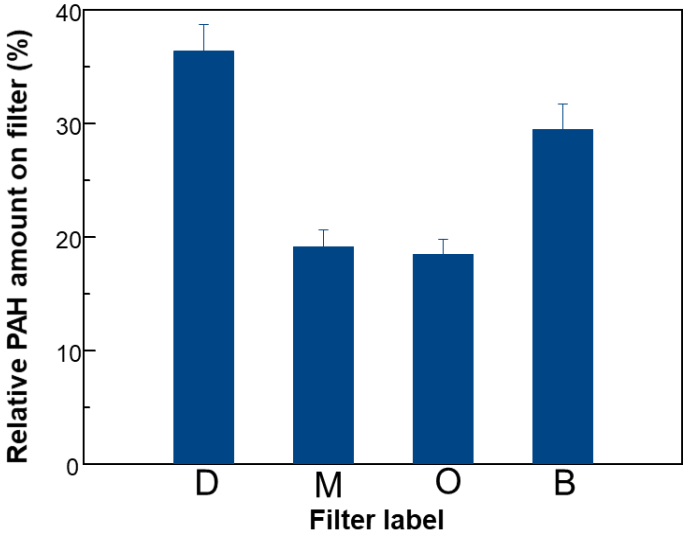

Figure 9. The figure above shows the distribution of PAH on each spot, which correlates to figure 7.

37mm Filter Distribution

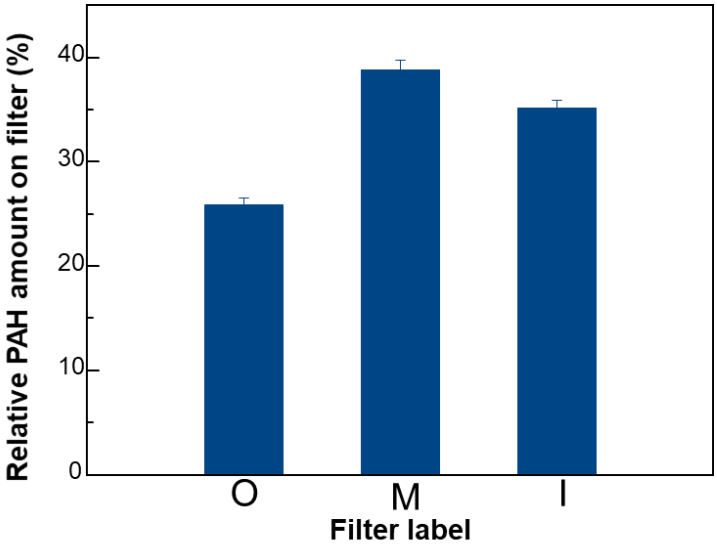

Figure 10. The figure above shows the distribution of PAH on each spot, which correlates to figure 8.

3.4.2. Live fire samples

On July 29, 2021, and August 1, 2021, PM sampling from live fires was conducted. The fire in July was conducted in Murfreesboro, TN, while the August fire was conducted in Mount Pleasant, TN. The July fire was conducted indoors where the smoke could not escape and was concentrated. The ambient temperature also reached much higher temperatures than the August fire, which was outdoors. Due to the high temperature, Firefighters could not tolerate standing near the fire for more than a few minutes. The temperature at the collection zone was around 400 °C, melting some equipment. Because of the high temperature and amount of smoke, the collection time for the July fire was around 10 minutes. Two pumps, A and B, were placed on tripods inside the building about 6 feet away from the fire, while two pumps, C and D were carried by Firefighters. The August fire was conducted outdoors with brush collected nearby. The temperature was much lower and could be tolerated for the Firefighters to stand nearby. Two pumps were carried by Firefighters, C and D, while one pump, B, was placed on a tripod about 10 feet away from the fire. This allowed for collection to last one hour. Figure 11 shows the amounts of PAH collected each day. As shown in figure 11, the filters collected during the July fire had much higher concentrations than the outdoor August fire. Filter A had by far the most PAHs. This is because filter A was inside the building during the fire, close enough that parts of its pump began to melt.

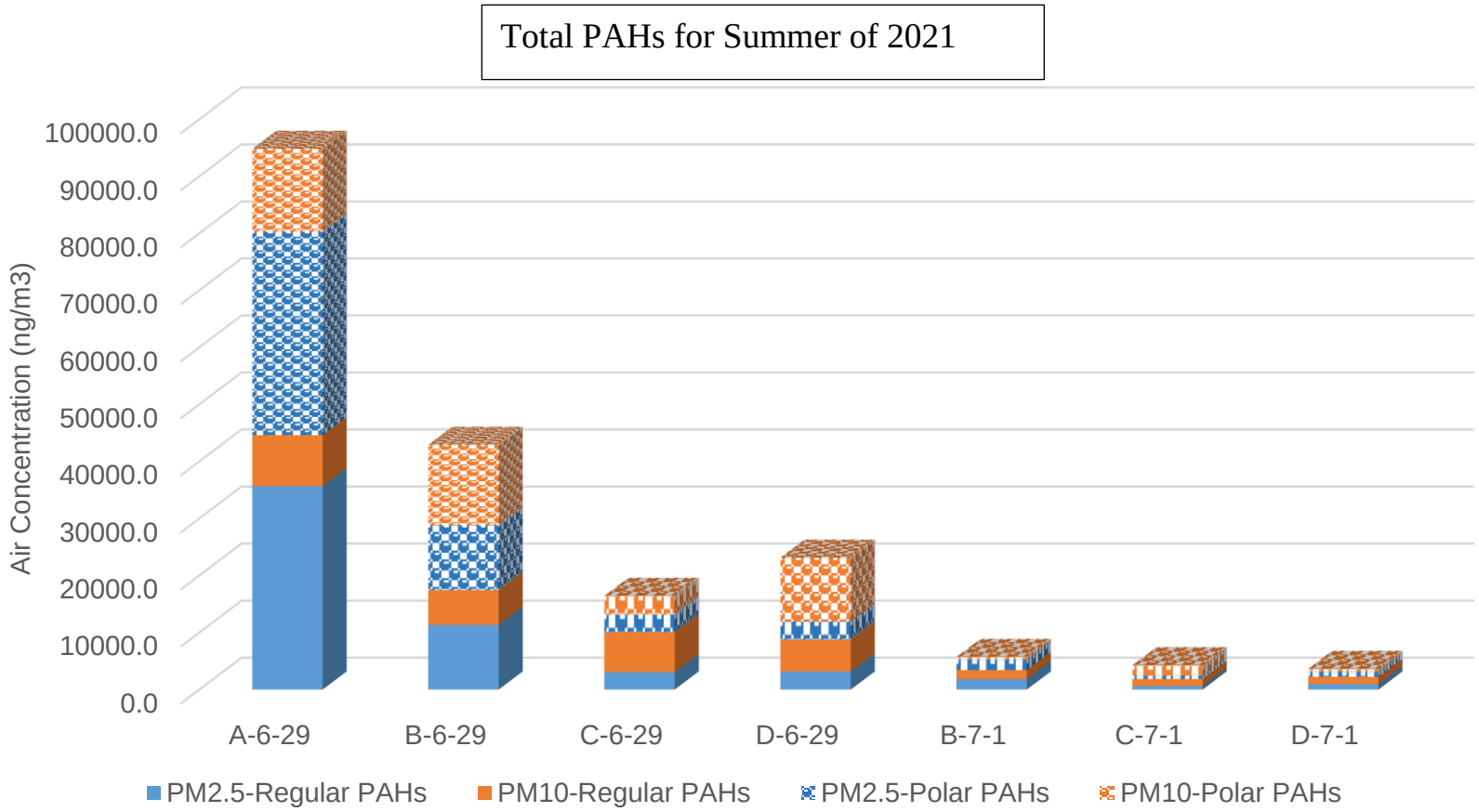

Figure 11. The figure above shows the concentration of PAH, both polar and non-polar on the filters for live burns that occurred on August 1 and July 29.

3.4.3 California fire samples

Samples were also collected from several wildfires in California in the fall of 2020 and the fall of 2021. These samples were analyzed with the same GC-MS method and extraction method detailed previously. During the fall of 2020 samples from two fires were analyzed, the Silverado fire and the Bond Fire. During the Silverado fire, two sites were sampled, as shown in figure 12. These are sites 1 and 2. The Bond fire had one sampling site listed in figure 12 as site 3. Site 1 was 4 miles from the edge of the Silverado Fire, while site 2 was 8 miles from the fire. Site 3 was 26.5 miles from the edge of the Bond fire. These samples were all collected on tripods in residential areas. Figure 13 shows the results of these collections. Figure 13A shows the total for each non-polar (regular) PAH found on all three filters at each site. Figure 13B shows the concentration of the non-polar PAH found on the $PM_{2.5}$ filters at each site. Figure 13C shows the concentration of the non-polar PAH found on the PM_{10} filters at each site, and figure 13D shows the concentrations of the non-polar PAH found on the $PM_{<10}$ filters at each site. Figure 14 shows the total combined non-polar PAH for each site. Site 3 had the highest amount of non-polar PAH among the three sites. The concentrations were high enough that samples collected over a month later still showed high amounts of non-polar PAH. Figure 15 shows the polar PAH concentrations for the fall 2020 fires. Figure 15A shows the total polar PAH concentration for each polar PAH analyzed. Figure 15B shows the concentration of the polar PAH found on the $PM_{2.5}$ filters at each site. Figure 15C shows the concentration of the polar PAH found on the PM_{10} filters at each site, and Figure 15D

shows the concentrations of the polar PAH found on the $PM_{<10}$ filters at each site. Figure 16 shows the total combined polar PAH for each site.

The fire collections during the summer of 2021 took place in the Trinity National Forest in California and were collected during the Monument fire. Collections took place on August 10, 2021, and September 13, 2021. During the August 2021 fire, samples were collected by firefighters who were wearing the collection pumps. During the September 2021 fire, samples were collected on tripods at the staging center. Because of this, the samples collected in August 2021 were exposed to severe smoke, while the September 2021 samples were only exposed to moderated smoke. Figure 17 shows the individual non-polar PAHs' concentrations for each PM size fraction and the total non-polar PAH (Figure 17A). Figure 17B is the $PM_{2.5}$ filter, while Figure 17C is the PM_{10} filter. Figure 17D is filter $PM_{<10}$. Figure 18 shows the similar plots of the total particulate matter and three particulate size fractions but for the analysis of polar PAHs (17.A total polar PAH, 17.B $PM_{2.5}$, 17.C PM_{10}, and 17.D $PM_{<10.}$). Figure 19 shows the total PAH for each sampling date for the summer of 2021. Several high molecular weight PAHs (5-6 fused benzene rings) such as benzo[k]fluoranthene, and benzo[a]pyrene were present at significantly high levels in PM samples during the first sampling event on Aug 10th, 2021; and their levels were much lower during the second sampling event. In addition, low molecular weight PAHs such as naphthalene exist at relatively low levels in most PM samples. It is worth noting that the higher molecular weight PAHs are usually of principal concern due to their recalcitrance, persistence, bioaccumulation, carcinogenicity, genotoxicity, and mutagenicity. A recent study on occupational exposure to PAHs of wildland firefighters at wildland fires reported the low level of high

molecular weight PAHs were detected in the gas samples, and our results indicate that the determination of particulate phase PAHs is also important, if not more, to the evaluation of PAHs exposure to firefighters.

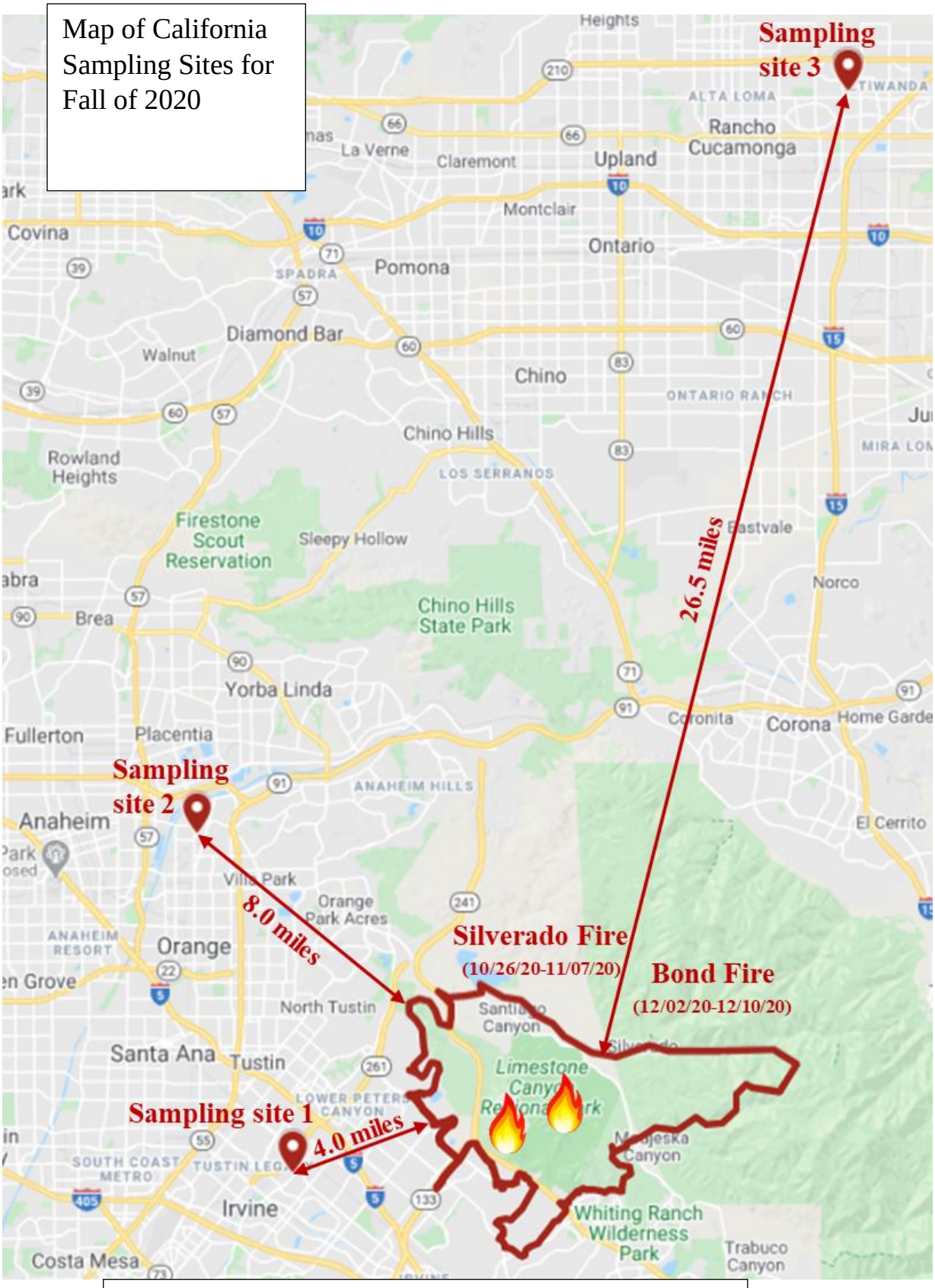

Figure 12. The figure above shows the sampling sites for the fall 2020 and the distances from the fires.

Individual Non-polar PAH Concentrations for Fall 2020

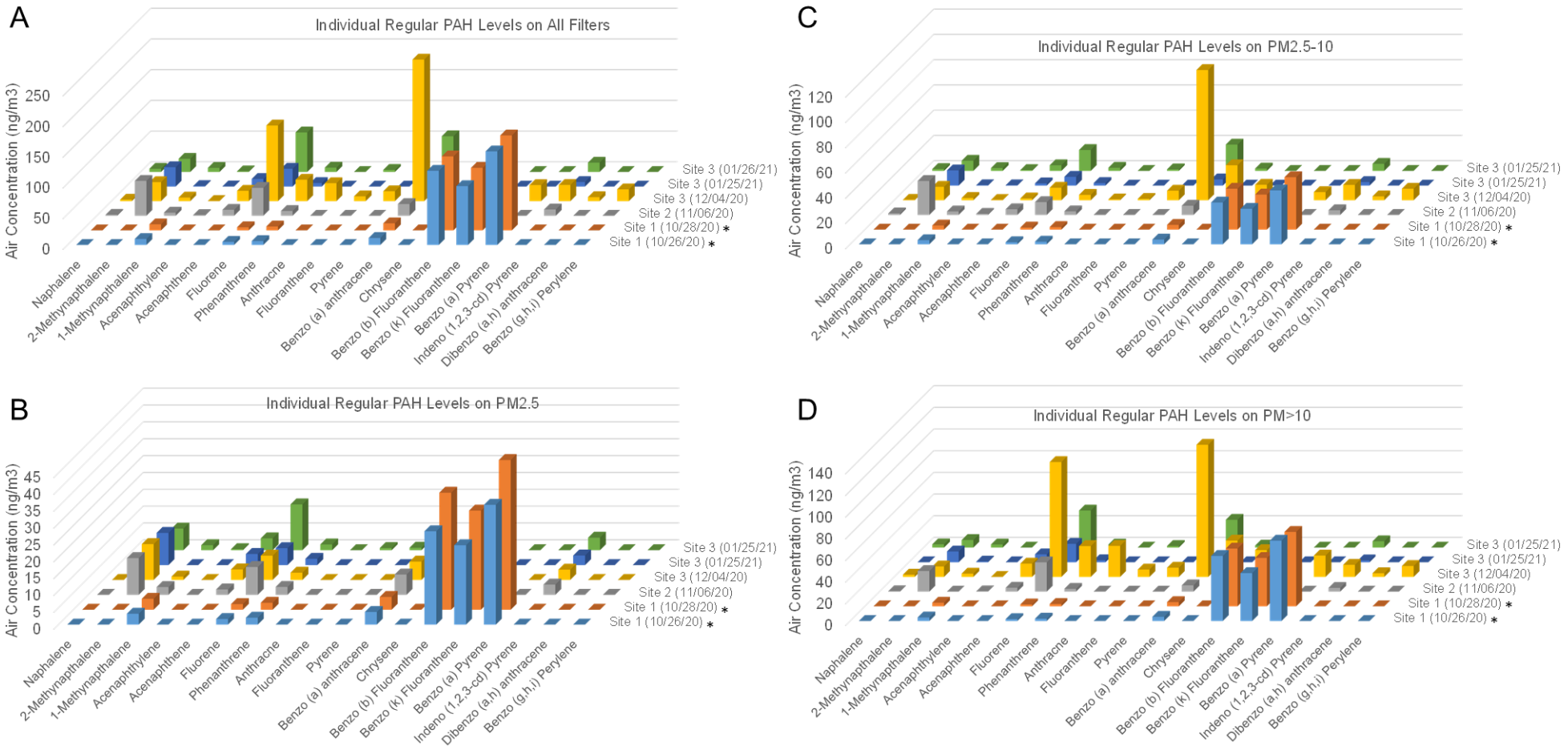

Figure 13. The figure above shows the total non-polar PAH found at each site (A), amount of PM2.5 (B), amount of PM10 (C), and the amount of >PM10 found at each site for the fall 2020 fires.

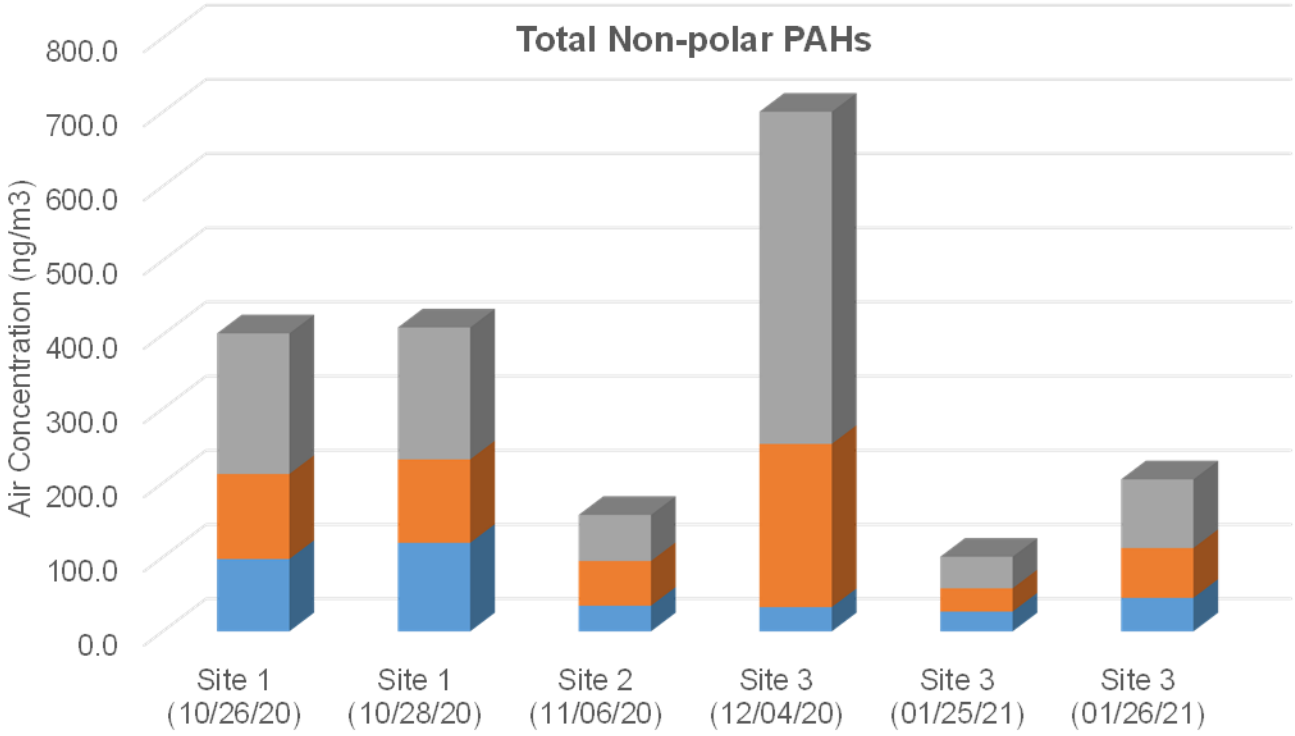

Figure 14. The figure above shows the total combined non-polar PAH for each sampling site for each day. Site 3 also had collections over month after the fire (1/25/21 and 1/26/21).

Individual Polar PAH Concentrations for Different PM Size Fractions for Samples Collected in Fall of 2020

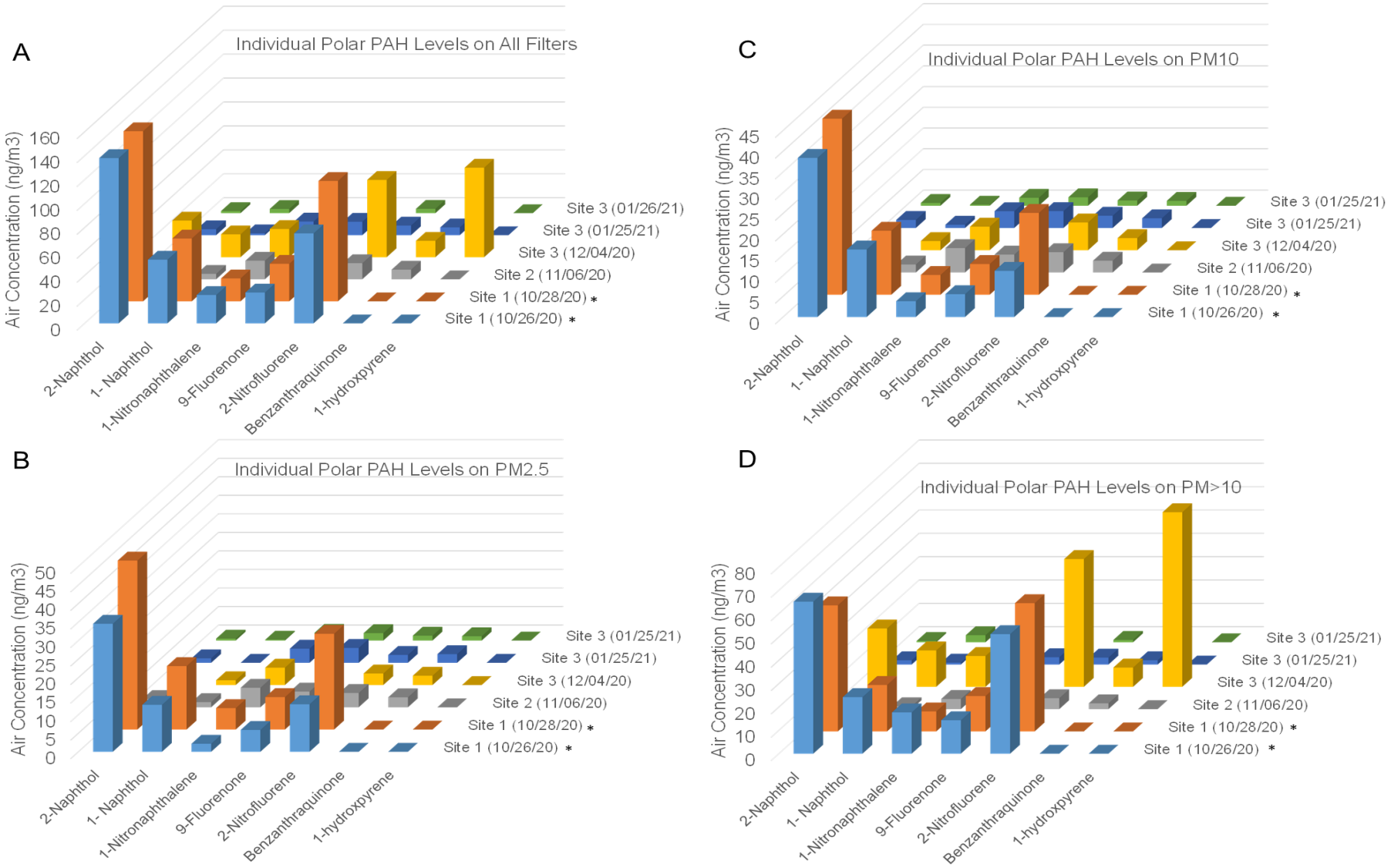

Figure 15. The figure above shows the total polar PAH found at each site (A), amount of PM2.5 (B), amount of PM10 (C), and the amount of >PM10 found at each site for the fall 2020 fires.

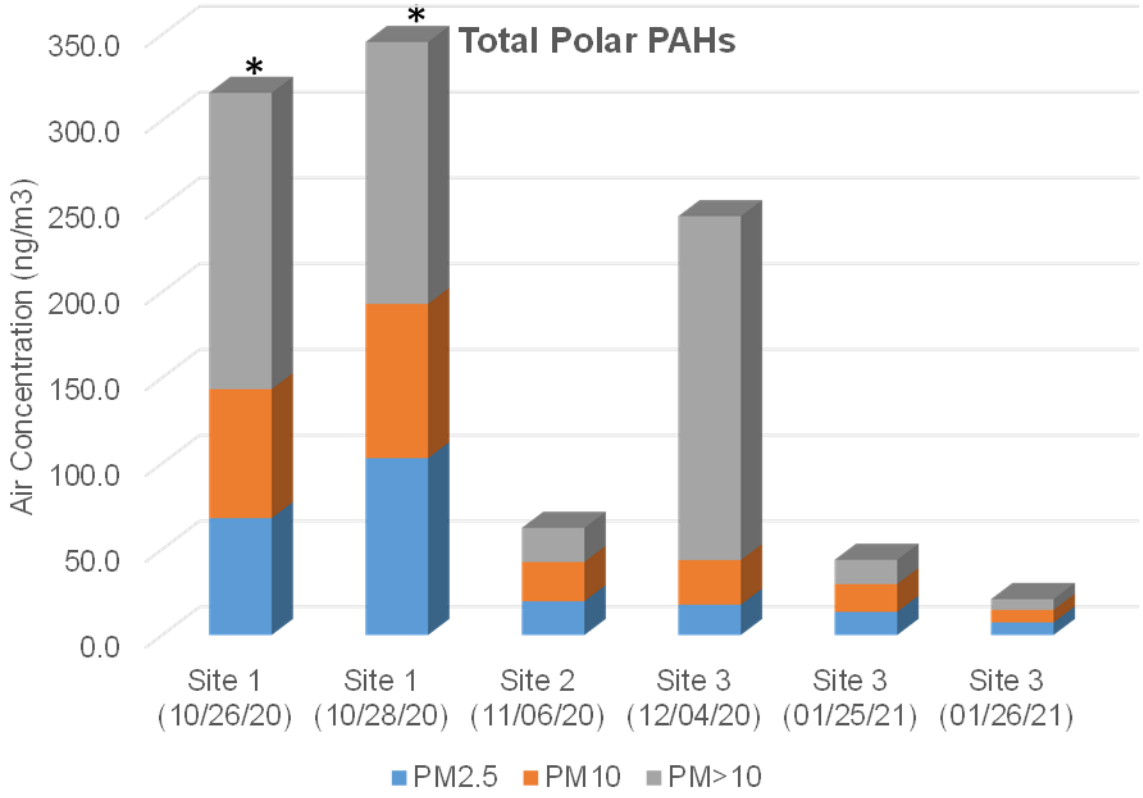

Figure 16. The figure above shows the total combined polar PAH for each sampling site for each day. Site 3 also had collections over month after the fire (1/25/21 and 1/26/21).

Individual non-polar PAH Concentrations for Summer 2021

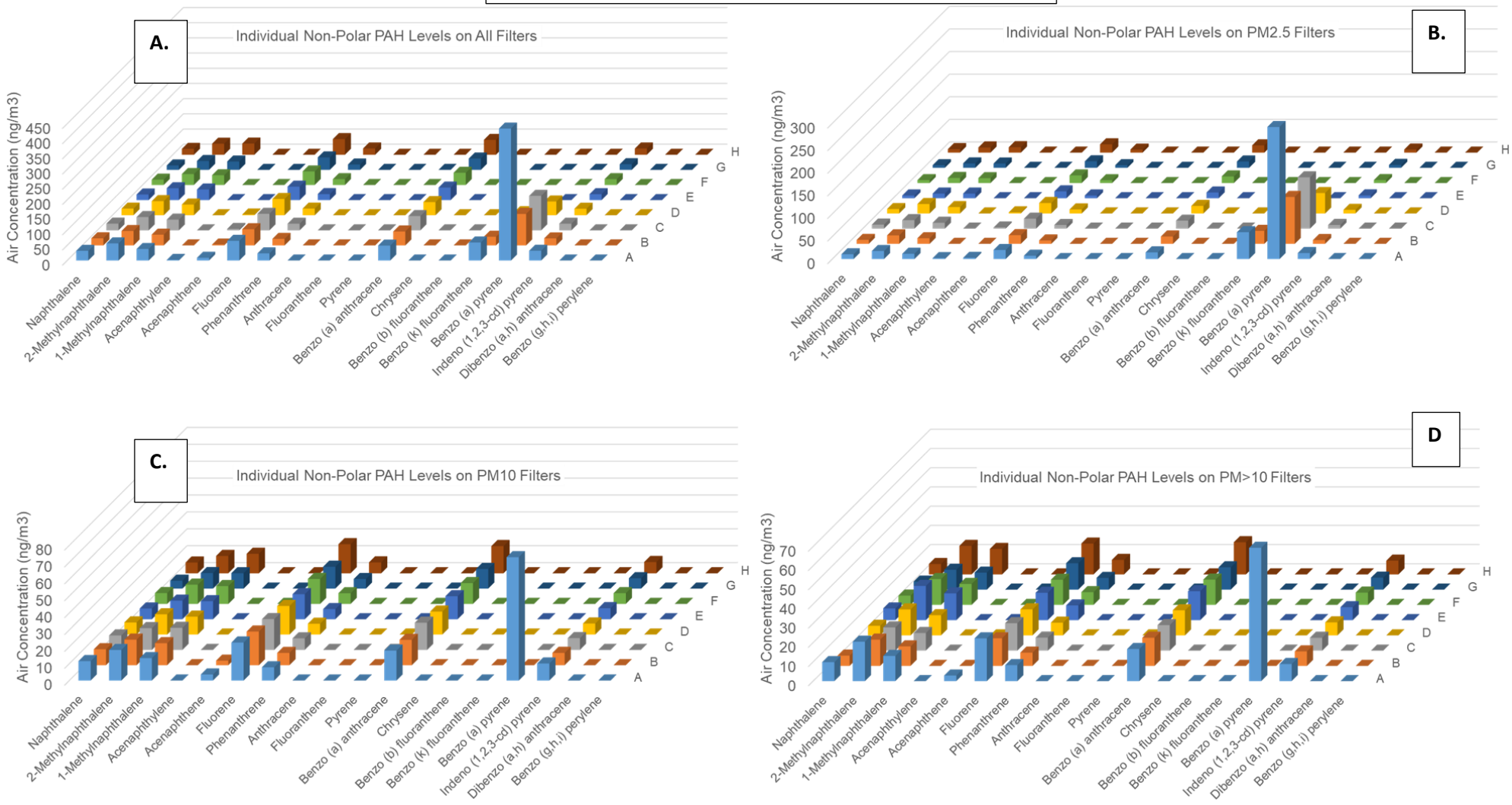

Figure 17. The figure above shows the total non-polar PAH found at each site (A), amount of $PM_{2.5}$ (B), amount of PM_{10} (C), and the amount of $PM_{<10}$ found at each site for the Summer 2021 fires.

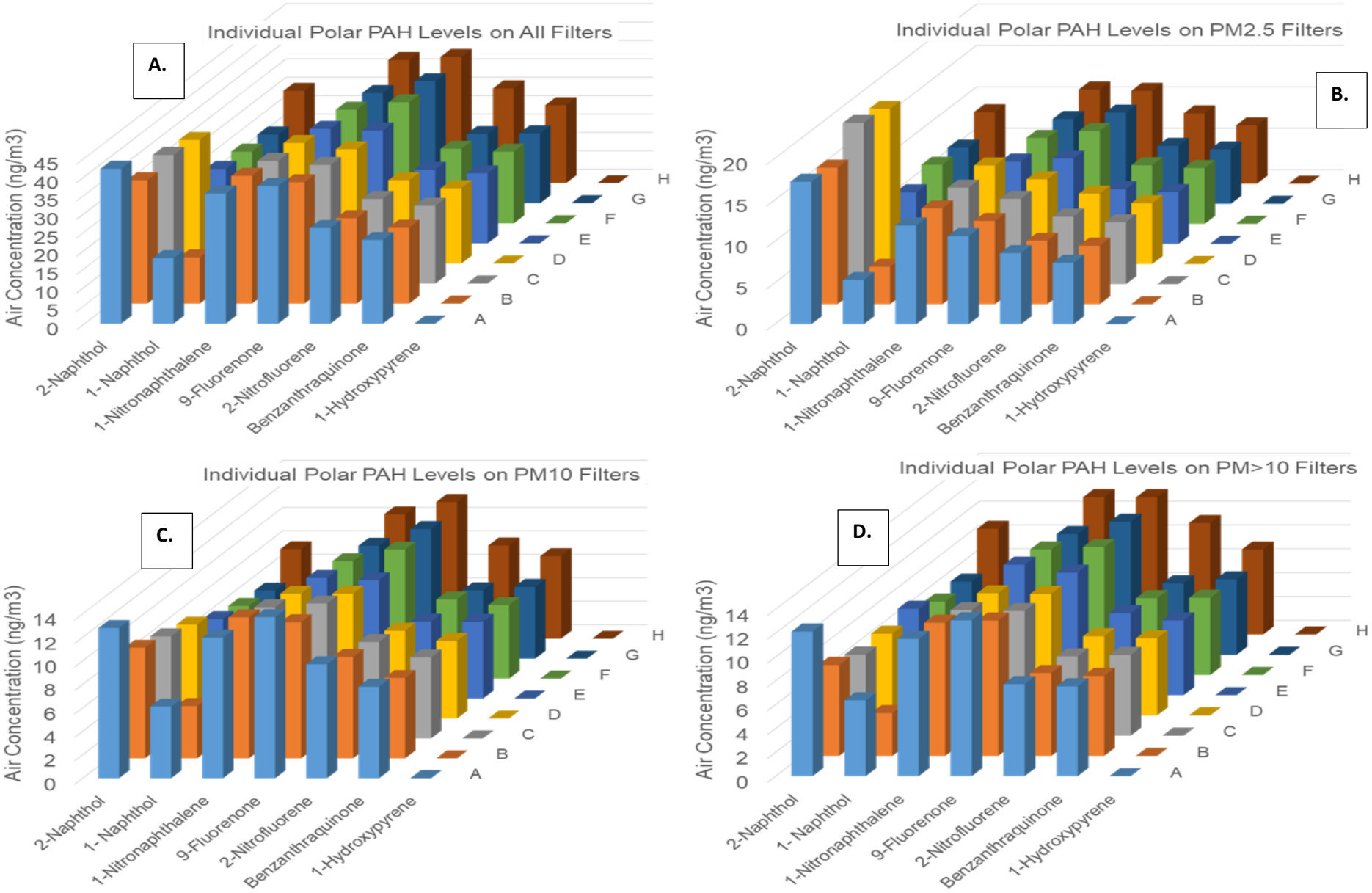

Figure 18. The figure above shows the total polar PAH found at each site (A), amount of $PM_{2.5}$ (B), amount of PM_{10} (C), and the amount of $PM_{<10}$ found at each site for the Summer 2021 fires.

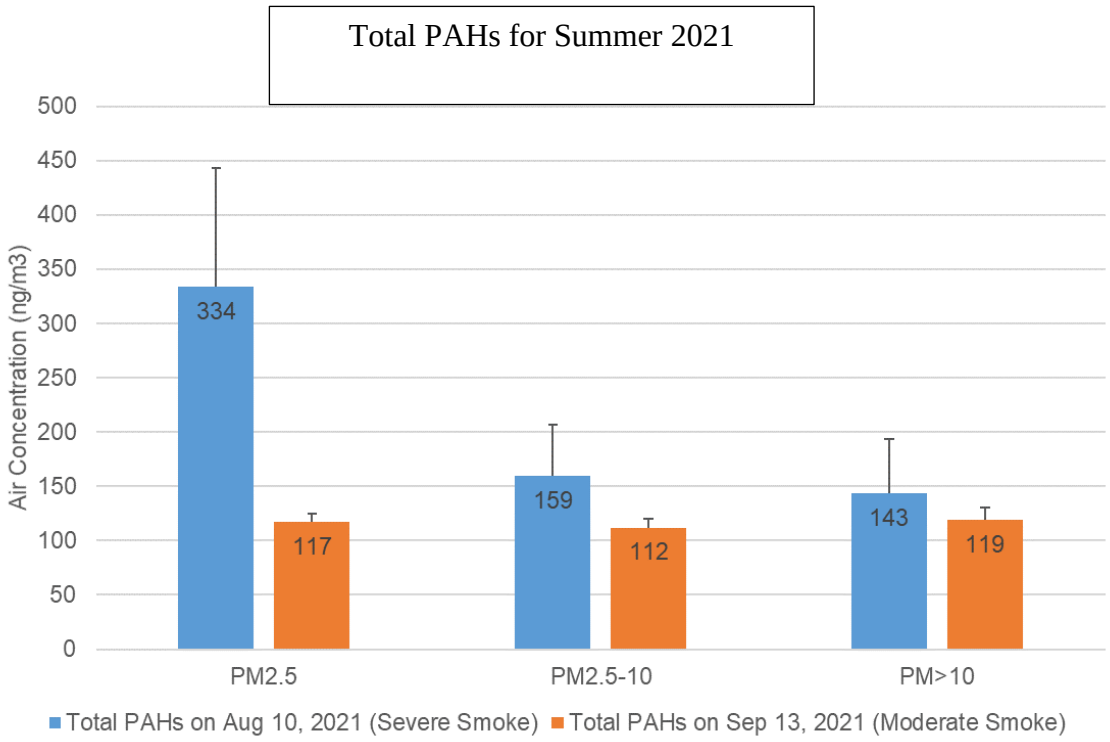

Figure 19. The figure above shows the total combined polar PAH for each sampling site, during the summer of 2021

3.5 Comparison between GC-MS and DART-MS

The GC-MS method was compared to the DART-MS method. The GC-MS method has a labor-intensive extraction process that takes a minimum of three hours to complete, while the DART-MS method takes less than ten minutes to prepare the sample for analysis. The GC-MS method takes over an hour to run a single analysis. The DART-MS method only takes six minutes to run one analysis. While the DART-MS method is both time-saving and less labor-intensive, it cannot separate isomers as seen in Figure 2. Because of this, it cannot separate half of the non-polar PAHs, while the GC-MS method can. The GC-MS and the DART-MS both have good R^2 values (Tables 7, 8, 15, and 16) for their respective regression equations, but the GC-MS has a larger dynamic range. The GC-MS method can detect down to 20 ng/mL. The DART-MS method can only detect down to 50 ng/mL. The recovery and precision are also better for the GC-MS. Tables 9 and 10 show that the typical accuracy is less than 10% relative error and that the precision is less than 14% RSD. DART-MS has worse accuracy and precision as seen in tables 16 and 17, with accuracy being as high as 33.1% relative error and precision being as high as 20.5% RSD. The GC-MS has a similar recovery rate as the DART-MS but with a lower standard deviation. This can be seen in tables 11, 12, 18, and 19. This can also be seen in the certified dust samples. The average recovery for the GC-MS was 104.3% and for DART-MS it was 103.9%. The standard deviation for the GC-MS was however half of what the DART-MS was. Tables 20 and 13 show that the GC-MS has an average standard deviation of 7.5 and that the DART-MS has an average of 15.2. The DART-MS is faster and less labor-intensive. It can also quantitatively detect as low as 50 ng/mL of non-polar PAH, but it is not as accurate or precise as the GC-MS method.

3.6 Heavy Metal Analysis

3.6.1 Calibration

A six-point calibration curve was created for 15 elements. Table 21 has a sample of these calibration curves along with the R^2 value and dynamic range. Mercury was not included in our study because the extraction method used (e.g., hot plate method and microwave digestion method) was inappropriate for mercury due to its volatility.

Table 21. The table below lists the selected heavy metals, a sample linear regression, R^2 value, and the dynamic range.

ICP-OES Sample Calibration		
Element Label	linear regression	R^2
Al	y=5312.12x-1558.7	0.999953
As	y=2903.646x-3.2485	0.999994
Be	y=3589910x+21000.27	0.999934
Co	y=46560.51x+179.4243	0.999976
Cr	y=56521.07x+159.8767	0.999983
Cu	y=58234.59x+261.5902	0.999995
Fe	y=91958.23x+2207.393	0.999975
Mn	y=348136.6x+2869.328	0.999925
Ni	y=28390.19x+190.4518	0.999958
Pb	y=6042.403x+48.34579	0.999982
Zn	y=78364.3x+1854.728	0.99998
Cd	y=108092.2x+227.6754	0.999973
Se	y=1096.67x+8.035829	0.999955
V	y=32825.78x-0.44113	0.999997

3.6.2 Comparison between microwave method and hot plate method

The two methods used for extracting the heavy metals from the filters were a microwave method and a hot plate method. The two methods are similar in the time that it takes to complete the extraction, however, it is much more labor-intensive to complete the hot plate method. This is because the microwave method can be left for an hour at a time for the microwave to do the extracting, but the hot plate method must be watched and adjusted by a person. In addition, the microwave digestion system can process 20 samples simultaneously, and the microwave method is also more efficient at extracting heavy metals than the hot plate method, as seen in
Table 22. The loss of metals by the hot plate method is likely caused during the time that the sample is being heated uncovered. Three samples of the same concentration were each extracted using either the hot plate method or the microwave method. The results show in Table 22 are the averages of these three samples for each method.

Table 22. The table below lists the selected element, the average percent recovery for the hot plate method, and the average percent recovery for the microwave method.

Hot Plate versus Microwave Method		
Element	Hot plate-Average %	Microwave-Average %
Al	84.6 ± 8	111.5±13
As	68.7±3	86.8±5
Be	76.7±3	84.9±2
Cd	70.0±3	79.4 ±3
Co	77.8±3	267.4±6
Cr	85.4±3	414.3±130
Cu	87.1±2	108.4±12
Fe	114.8±17	345.9±50
Mn	79.8±3	84.3±1
Ni	75.4±3	84.8±3
Pb	72.3±3	82.4±2
Se	70.8±11	99.7±4
V	86.2±3	92.8±0.4
Zn	68.8±9	85.7±11

3.6.3 Filter samples

Heavy metals were extracted from the filters from the Monument fire in California with the microwave extraction method. Six filters were analyzed for heavy metal concentration. The results are shown in table 23. Four of the samples were $PM_{2.5}$, which tended to have more heavy metal than the $PM_{<10}$ filters. The other two samples were $PM_{<10}$. Lead and Chromium had relatively high concentrations as they are both considered concerning pollutants.

Table 23. The table below list six filters heavy metal concentrations as well as the total metal concentration from the Monument fire in California.

ICP-OES Filter Results												
Filter	Al ($\mu g/m^3$)	Cd ($\mu g/m^3$)	Co ($\mu g/m^3$)	Cr ($\mu g/m^3$)	Cu ($\mu g/m^3$)	Fe ($\mu g/m^3$)	Mn ($\mu g/m^3$)	Ni ($\mu g/m^3$)	Pb ($\mu g/m^3$)	V ($\mu g/m^3$)	Zn ($\mu g/m^3$)	Total metal
$PM_{2.5}$-1	5.5	0	0	1.0	1.2	10.4	1.0	0.2	0.2	0	0.48	20.0
$PM_{2.5}$-2	24.8	0.02	0.06	11.0	1.0	58.7	6.4	1.3	12.4	0.15	1.45	117.4
$PM_{2.5}$-3	5.2	0	0	3.0	0.7	17.4	1.9	0.4	0.1	0	0.3	28.9
$PM_{2.5}$-4	4.2	0	0	0.1	0.6	4.6	0.4	0.1	0.1	0	0.24	10.4
$PM_{<10}$-2	15.2	0	0	5.3	0.7	31.2	3.2	0.8	0.2	0	0.79	57.3
$PM_{<10}$-3	5.8	0	0	2.8	0.5	18.2	1.8	0.4	0.1	0	0.18	29.7

CHAPTER FOUR: CONCLUSION

Eighteen non-polar PAHs and seven polar PAHs were studied in $PM_{2.5}$ and $PM_{<10}$ from wildfire smoke and prescribed burns. The wildfire smoke was collected during the falls of 2020 and 2021 in California, and the prescribed burns were collected in the summer of 2021 in Middle Tennessee. During the prescribed indoor burn in Murfreesboro TN, high levels of PAHs were detected from all of the sampling devices, but the sampling devices that were stationary inside the structure collected significantly higher amounts of both polar and non-polar PAHs. While the prescribed burn in Middle Tennessee that occurred outdoors had much lower PAH concentrations collected than the indoor burn, due to the smoke dissipating in the open air, both polar and non-polar PAH were detected in significant amounts.

PAHs were detected in all of the California live-fire samples. The concentrations collected correlated with the wildfire events nearby. The closer a sample was collected to the wildfire, the higher the concentration of PAH tended to be. The California samples collected by Firefighters during the fighting of the fire had the highest amount of PAH.

The wildfire samples were all analyzed using the traditional method of gas chromatography-mass spectrometry. This method involves a labor-intensive extraction and a long analysis period. A novel method of analyzing both polar and non-polar PAH is direct analysis in real-time mass spectrometry. DART-MS is much faster than GC-MS

and does not involve an extraction process. The DART-MS method described takes less than seven minutes to complete an analysis. It also can adequately quantitate both polar and non-polar PAH with unique characteristic ions. The DART-MS, however, cannot resolve isomeric PAHs, where the GC-MS can. The DART-MS is also less accurate, precise than the GC-MS method.

The ICP-OES was able to identify and quantify heavy metals quickly and efficiently. The extraction process was, however, longer. Two extraction methods were tested for efficiency, ease of performing, and speed. While both methods took between two and three hours to complete, the hot plate method described was labor-intensive and less efficient than the microwave extraction method, making it the preferred method.

CHAPTER FIVE: REFERENCES

1. (2020). National Interagency Coordination Center "National Interagency Coordination Center Wildland Fire Summary and Statistics Annual Report" 2020. National Interagency Coordination Center. https://www.predictiveservices.nifc.gov/intelligence/2020_statssumm/annual_report_2020.pdf. Accessed 09/15/2021
2. Navarro, K. M., Clark, K. A., Hardt, D. J., Reid, C. E., Lahm, P. W., Domitrovich, J. W., Butler, C. R., and Balmes, J. R. (2021) "Wildland firefighter exposure to smoke and COVID-19: A new risk on the fire line". *Science of the Total Environment 760*.
3. Air Quality Planning & Science Division. (2021). "Camp Fire Air Quality Data Analysis". California Air Resources Board.
4. Office of Air and Radiation. (2003). "Particle Pollution and Your Health". EPA.
5. Bølling, A. K., Pagels, J., Yttri, K. E., Barregard, L., Sallsten, G., Schwarze, P. E., and Boman, C. (2009) "Health effects of residential wood smoke particles: the importance of combustion conditions and physicochemical particle properties". *Particle and Fibre Toxicology 6*.
6. Hwang, J., Taylor, R., Cann, C., Norris, P., and Golla, V. (2019) "Evaluation of Accumulated Polycyclic Aromatic Hydrocarbons and Asbestiform Fibers on Firefighter Vehicles: Pilot Study". *Fire Technology 55*, 2195–2213.

7. Adetona, O., Simpson, C., Onstad, G., and Naeher, L. (2013) “Exposure of Wildland Firefighters to Carbon Monoxide, Fine Particles, and Levoglucosan”. *The Annals of Occupational Hygiene 57*, 979–991.
8. U.S. Army Natick Soldier Research, Development, and Engineering Center. (2014). “Wildland Firefighter Personal Protective Equipment (PPE) Selection Guide”. Homeland Security.
9. Tian, Y., Liu, H., Wu, Y., Si, Y., Li, M., Wu, Y., Wang, X., Wang, M., Chen, L., Wei, C., Wu, T., Gao, P., and Hu, Y. (2019) “Ambient particulate matter pollution and adult hospital admissions for pneumonia in urban China: A national time series analysis for 2014 through 2017”. *PLOS Medicine 16*.
10. Migliaccio, C. T., Kobos, E., King, Q. O., Porter, V., Jessop, F., and Ward, T. (2013) “Adverse effects of wood smoke PM2.5 exposure on macrophage functions”. *Inhalation Toxicology 25*, 67–76.
11. Kim, Ki-Hyun, AraJahan, Shamin, Kabir, Ehsanul, Brown, Richard, J.C., A Review of Airborne Polycyclic Aromatic Hydrocarbons (PAHs) and their Human Health Effects." *Environment International* 60 (2013): 71-80.
12. Salwa Kamal Hassan. "Particle-Bound Polycyclic Aromatic Hydrocarbon in the Atmosphere of Heavy Traffic Areas in Greater Cairo, Egypt: Status, Source, and Human Health Risk Assessment." *Atmosphere* 9.10 (2018)
13. Kameda Y, Shirai J, Komai T, Nakanishi J, Masunaga S. “Atmospheric polycyclic aromatic hydrocarbons: size distribution, estimation of their risk and their depositions to human respiratory tract.” Sci Total Environment 2005;340:71–80.

14. Ray S, Khillare PS, Kim KH, Brown RJC. “Distribution, sources, and association of polycyclic aromatic hydrocarbons, black carbon, and total organic carbon in size-segregated soil samples along a background-urban–rural transect”. Environ Eng Sci 2012;29: 1008–19.

15. Babić, J., Vidakovic, S., Skalijac, S., Kartalovic, B., Ljubojevic, B., Cirkovic, M., Teodorovic, V., "Factors Affecting Elimination of Polycyclic Aromatic Hydrocarbons from Traditional Smoked Common Carp Meat." *IOP Conference Series.Earth and Environmental Science* 85.1 (2017)

16. Mehlman, M. A., Mumtaz, M. M., Farron, O., & Rosa, C. T. (1997). “Health Effects of Polycyclic Aromatic Hydrocarbons”. *J. Clean Technol. Environ. Toxicol. Med., 6(1), 1–22.*

17. Thyssen J, Althoff J, Kimmerle G, Mohr U. “Inhalation studies with benzo[a]pyrene in Syrian golden hamsters”. J Natl Cancer Inst. 1981 Mar;66(3):575-7. PMID: 6937711.

18. Irikura, Beth. "*Arabidopsis* Response to the Carcinogen Benzo[a]Pyrene." Ph.D. University of Hawai'i at Manoa, 2008. United States -- Hawaii: *ProQuest Dissertations & Theses Global.* Web1

19. United Kingdom. PHE Centre for Radiation, Chemical and Environmental Hazards or Radiation, Chemical and Environmental Hazards. “Polycyclic Aromatic Hydrocarbons (Benzo[a]Pyrene)” *Toxicological Overview*, Aug. 2018. assets.publishing.service.gov.uk/government/uploads/system/uploads/attachment_data/file/737017/PAH_TO_PHE_240818.pdf#:~:text=PAHs%20typically%20occ

ur%20in%20complex%20mixtures%20and%20not,absorption%20are%20the%20main%20routes%20of%20occupational%20exposure. Accessed Sept. 15, 2021

20. United States, Congress, Office of Solid Waste. “Polycyclic Aromatic Hydrocarbons (PAHs)”, EPA, Jan. 2008. archive.epa.gov/epawaste/hazard/wastemin/web/pdf/pahs.pdf.
21. Hwang, Jooyeon, et al. "Evaluation of Accumulated Polycyclic Aromatic Hydrocarbons and Asbestiform Fibers on Firefighter Vehicles: Pilot Study." *Fire technology* 55.6 (2019): 2195-213. *ABI/INFORM Collection.* Web.
22. Pereira, P., and Úbeda, X.. "Spatial Distribution of Heavy Metals Released from Ashes After a Wildfire." *Journal of Environmental Engineering and Landscape Management* 18.1 (2010): 13-22. Web.
23. Suprapto, D., S. Suryanti, and N. Latifah. "Content Heavy Metal Pb, Cd in Perna Viridis and Sediments in Semarang Bay." *IOP Conference Series.Earth and Environmental Science* 116.1 (2018) Publicly Available Content Database. Web.
24. Van de Mortel, Judith Elisabeth. "Heavy Metal Tolerance and Accumulation in Thlaspi Caerulescens, a Heavy Metal Hyperaccumulating Plant Species = Zware Metalen Tolerantie En Accumulatie in Thlaspi Caerulescens, Een Zware Metalen Hyperaccumulerende Plantensoort." Ph.D. Wageningen University and Research, 2007. Netherlands: ProQuest Dissertations & Theses Global. Web.
25. Jaishankar, Monisha, et al. “Toxicity, Mechanism and Health Effects of Some Heavy Metals.” *Interdisciplinary Toxicology*, vol. 7, no. 2, 2014, pp. 60–72., doi:10.2478/intox-2014-0009.

26. Haley BE. “Mercury toxicity: genetic susceptibility and synergistic effects”. *Medical Veritas.* 2005;2(2):535–42.

27. Christensen, A., C. Östman, and R. Westerholm. "Ultrasound-Assisted Extraction and on-Line LC-GC-MS for Determination of Polycyclic Aromatic Hydrocarbons (PAH) in Urban Dust and Diesel Particulate Matter." *Analytical and Bioanalytical Chemistry* 381.6 (2005): 1206-16. Web.

28. EPA. (1984). *Method 610: “*Polynuclear aromatic hydrocarbons*”*. EPA. Retrieved October 8, 2021, from https://beta.epa.gov/sites/default/files/2015-10/documents/method_610_1984.pdf. Accessed Sept. 30, 2021

29. EPA. (1999, January). “Compendium Method TO-13A Determination of Polycyclic Aromatic Hydrocarbons (PAHs) in Ambient Air Using Gas Chromatography/Mass Spectrometry (GC/MS)”. Compendium of Methods for the Determination of Toxic Organic Compounds in Ambient Air. Retrieved from https://www.epa.gov/sites/default/files/2019-11/documents/to-13arr.pdf#:~:text=%20%20%20Title%20%20%20Method%20TO-13A,%20Thursday%2C%20March%2018%2C%201999%209%3A44%3A05%20AM%20. Accessed Oct. 1, 2021

30. National Institute for Occupational Safety and Health, “POLYNUCLEAR AROMATIC HYDROCARBONS by GC” (1994). NIOSH.

31. Wang, Xiaoyu, et al. "Sensitive and Selective Determination of Polycyclic Aromatic Hydrocarbons in Mainstream Cigarette Smoke using a Graphene-Coated Solid-Phase Microextraction Fiber Prior to GC/MS." *Talanta* 140 (2015): 102-8. Web.

32. Gross, J. H. "Direct Analysis in Real Time-a Critical Review on DART-MS." *Analytical and Bioanalytical Chemistry* 406.- (2014): 63-80. Web.

33. Zhao, Y., Fairhurst, M. C., Wingen, L. M., Perraud, V., Ezell, M. J., & Finlayson-Pitts, B. (2017). New insights into atmospherically relevant reaction systems using direct analysis in real-time mass spectrometry (DART-MS). *Atmospheric Measurement Techniques, 10*(4), 1373-1386. http://dx.doi.org/10.5194/amt-10-1373-2017

34. Drury, N., Ramotowski, R., & Moini, M. (2018). A comparison between DART-MS and DSA-MS in the forensic analysis of writing inks. *Forensic Science International (Online), 289*, 27-32. http://dx.doi.org/10.1016/j.forsciint.2018.05.009

35. Sisco, E., & Forbes, T. P. (2021). Forensic applications of Dart-MS: A review of recent literature. *Forensic Chemistry, 22*, 100294. https://doi.org/10.1016/j.forc.2020.100294

36. Al-Onazi, W., Al-Mohaimeed, A., Amina, M., & El-Tohamy, M. (2021). Identification of chemical composition and metal determination of 0RW1S34RfeSDcfkexd09rT2retama raetam1RW1S34RfeSDcfkexd09rT2 (forssk) stem constituents using ICP-MS, GC-MS-MS, and DART-MS. *Journal of Analytical Methods in Chemistry, 2021*http://dx.doi.org/10.1155/2021/6667238